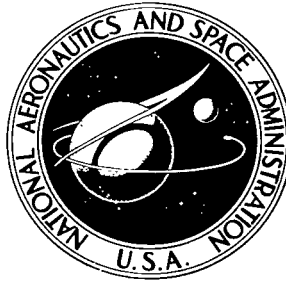


NASA TECHNICAL NOTE



NASA TN D-5144

C.1

NASA TN D-5144



LOAN COPY: RETURN TO
AFWL (WLIL-2)
KIRTLAND AFB, N MEX

A PARAMETRIC ANALYSIS OF SURFACE TEMPERATURES OF PARABOLOIDAL SOLAR CONCENTRATORS IN SPACE

by Robert J. Platt, Jr.
Langley Research Center
Langley Station, Hampton, Va.



A PARAMETRIC ANALYSIS OF SURFACE TEMPERATURES OF
PARABOLOIDAL SOLAR CONCENTRATORS IN SPACE

By Robert J. Platt, Jr.

Langley Research Center
Langley Station, Hampton, Va.

NATIONAL AERONAUTICS AND SPACE ADMINISTRATION

For sale by the Clearinghouse for Federal Scientific and Technical Information
Springfield, Virginia 22151 - CFSTI price \$3.00

A PARAMETRIC ANALYSIS OF SURFACE TEMPERATURES OF PARABOLOIDAL SOLAR CONCENTRATORS IN SPACE

By Robert J. Platt, Jr.
Langley Research Center

SUMMARY

A parametric analysis has been made of the surface temperatures of a paraboloidal mirror in space and aimed at the sun. The problem is simplified by the assumption of steady-state conditions, the paraboloidal mirror (solar concentrator) being located directly between the earth and the sun. Surface temperatures are plotted for a range of the important parameters for altitudes up to 35 000 kilometers. Additional temperature plots are presented for the case of a solar concentrator approaching the sun.

The results indicate that at an irradiance of one solar constant, a concentrator of very low thermal conductance may experience a front surface temperature of 600° K in space, unless a front surface coating is used to increase the emittance. The temperature difference between the front and rear surfaces, which causes thermal distortion of the mirror, may be greatly reduced by proper selection of thermal control surfaces if the concentrator is near the earth. At irradiances of many solar constants, as in the case of a concentrator used with a solar probe, metal construction and high emittance coatings appear to be needed to reduce the front-surface temperature and to minimize thermal distortion.

INTRODUCTION

Several types of proposed space solar-power systems require elevated temperatures for efficient operation. The solar energy must be concentrated by some form of lens or mirror in order to obtain the needed high temperature at the heat-absorber location. An efficient way of obtaining this high temperature is with a paraboloidal mirror, which may be constructed of materials ranging from thin metals to much thicker plastic foams. (See ref. 1.) Of interest to the designer of such a space power system is the temperature of the paraboloidal concentrator itself, for the temperature limit of the structural material used may possibly be exceeded. Even if the physical properties of the material are not seriously affected, temperature gradients tend to distort the shape of the mirror and degrade its concentrating ability. A method for computing this thermal

distortion of a paraboloidal shell is given in reference 2. However, it is necessary to know the concentrator front and rear surface temperatures before the distortion can be computed.

A parametric analysis of the surface temperatures of paraboloidal mirrors has been undertaken in order to indicate the role of the various parameters involved, and as an aid in the design of such concentrators. Two space environments have been considered: the first representing a solar concentrator in earth orbit and the second, part of a solar probe. The first case is complicated by the fact that the heat inputs from both the sun and the earth change with time. Although it is possible to compute the concentrator temperatures as a function of time (see refs. 3 and 4), the labor required makes it impractical for a parametric analysis. The near-earth case has therefore been simplified by considering only steady-state conditions, with the paraboloidal shell, which forms the concentrator, aimed at the sun and located on a line between the center of the sun and the earth. This chosen orbital position results in the maximum overall heat input to the concentrator because, in this position, the rear surface intercepts the maximum amount of heat from the earth. Therefore, the temperatures presented herein will approximate the highest to be expected on a solar concentrator in earth orbit, but will underestimate the maximum temperature difference between the front and rear surfaces.

For the near-earth case, the parameters which are varied are the emittances and absorptances of the front and rear surfaces, the thermal conductance of the mirror, and the altitude. For the solar-probe case, the parameters varied are the solar absorptance of the front surface, the emittances of both surfaces, the thermal conductance of the mirror, and the irradiance on the mirror expressed in solar constants.

SYMBOLS

A	surface area of concentrator, meter ²
a	average albedo of earth
dA	elementary area at center of concentrator, meter ²
E _a	irradiance on concentrator due to earth albedo, watts/meter ²
E _e	irradiance on concentrator due to earth reradiation, watts/meter ²
E _m	irradiance on concentrator due to reradiation from mirror surface, watts/meter ²

E_S	irradiance on concentrator due to direct solar radiation, watts/meter ²
$F_{A_1 \rightarrow dA}$	configuration factor from A_1 to dA
$F_{dA \rightarrow A_1}$	configuration factor from dA to A_1
$F_{dA \rightarrow D_R}$	configuration factor from dA to disk D_R circumscribed by rim of paraboloid
$F_{D_e \rightarrow dA}$	configuration factor from disk which represents the earth to dA
$F_{dA \rightarrow D_e}$	configuration factor from dA to disk D_e which represents the earth
h	altitude, kilometers
k	thermal conductivity, watts/meter-degree Kelvin
r_e	radius of earth, kilometers
r_d	radius of disk (see fig. 23), meters
T	absolute temperature, degrees Kelvin
t	thickness of paraboloidal concentrator, meters
α	solar absorptance
β_R	angle of paraboloid indicated in figure 22, degrees
ϵ	total hemispherical emittance
θ_R	rim angle of paraboloidal concentrator, degrees (fig. 22)
σ	Stefan-Boltzmann constant, 5.6697×10^{-8} watt/meter ² -degree Kelvin ⁴
φ	angle indicated in figure 23, degrees

Subscripts:

- 1 front surface of concentrator
- 2 rear surface of concentrator

METHOD OF ANALYSIS

Near-Earth Environment

A paraboloidal mirror in space, aimed at the sun, will receive direct radiation from the sun on its front surface and may receive additional radiation from the earth on either surface. For an orbiting mirror, these heat inputs vary with time. A further complication is that a radial temperature gradient may exist because, for instance, of the radially changing angle of incidence between the solar radiation and the paraboloidal surface. In the present analysis the problem has been simplified to treat the steady-state condition of a paraboloidal mirror aimed at the sun and located between the sun and the earth. (See fig. 1.) The surface temperatures are computed for an elementary area of the concentrator, of thickness t , located near the axis of the concentrator. Further simplifying assumptions are:

- (1) The concentrator is unshadowed
- (2) The earth reflects diffusely 35 percent of the intercepted solar radiation without changing its spectral distribution. The remaining 65 percent is reemitted uniformly, as would occur if the earth were replaced by a black body at a uniform temperature
- (3) Absorptance of a concentrator surface for thermal radiation emitted from either the concentrator or the earth is equal to the hemispherical emittance of the surface
- (4) Heat conduction through the paraboloidal concentrator is one-dimensional (from one surface to the opposite surface with no radial flow)
- (5) Reflection from the front surface is completely specular
- (6) For the purpose of computing the reradiation from the front surface to the central element, the temperature of the front surface is assumed to be uniform.

Consider a mirror located between the earth and the sun and aimed at the sun (fig. 1). For the assumed steady-state condition, the heat absorbed by the front surface, made up of the absorption of direct solar energy plus the absorption of heat reradiated from the mirror itself, is equal to the heat emitted from the front surface plus the heat conducted to the rear surface. For a centrally located elementary area of the mirror, this heat balance may be expressed as

$$\alpha_1 E_S + \epsilon_1 E_m = \epsilon_1 \sigma T_1^4 + \frac{k}{t}(T_1 - T_2)$$

An expression for E_m , derived in appendix A for a paraboloidal mirror, is

$$E_m = \epsilon_1 \sigma T_1^4 \left(\frac{\tan^2 \frac{\theta_R}{2}}{4 + \tan^2 \frac{\theta_R}{2}} \right)$$

By substitution,

$$\alpha_1 E_S + \epsilon_1^2 \sigma T_1^4 \left(\frac{\tan^2 \frac{\theta_R}{2}}{4 + \tan^2 \frac{\theta_R}{2}} \right) = \epsilon_1 \sigma T_1^4 + \frac{k}{t}(T_1 - T_2) \quad (1)$$

The heat absorbed by the rear surface, made up of both reradiated energy and albedo from the earth plus the heat conducted from the front surface to the rear surface, is equal to the heat emitted from the rear surface. For a centrally located elementary area of the rear surface, this heat balance may be expressed as

$$\epsilon_2 E_e + \alpha_2 E_a + \frac{k}{t}(T_1 - T_2) = \epsilon_2 \sigma T_2^4$$

An expression for E_e , derived in appendix B, is

$$E_e = \frac{(1 - a)E_S}{4 \left(1 + \frac{h}{r_e}\right)^2}$$

An approximate expression for E_a , derived in appendix C, is

$$E_a = \frac{aE_S}{\left(1 + \frac{h}{r_e}\right)^2}$$

By substitution,

$$\frac{\epsilon_2(1 - a)E_S}{4 \left(1 + \frac{h}{r_e}\right)^2} + \frac{\alpha_2 a E_S}{\left(1 + \frac{h}{r_e}\right)^2} + \frac{k}{t}(T_1 - T_2) = \epsilon_2 \sigma T_2^4 \quad (2)$$

The surface temperatures T_1 and T_2 may be found from equations (1) and (2) if values of the parameters are known or assumed. These temperatures were obtained by means of a digital computer for a range of values of α_1 , α_2 , ϵ_1 , ϵ_2 , k/t , and h . The value of E_s was taken as 1 solar constant or 1400 watts/meter². The computations were carried out only for a paraboloid with a rim angle θ_R of 60° since this angle is representative of present solar concentrators and because the temperature of the concentrator is not strongly influenced by the rim angle.

Solar-Probe Environment

The analysis of the surface temperatures of a paraboloidal mirror approaching the sun is similar to that of the near-earth case except that the direct irradiance on the front surface due to the sun becomes a variable and the rear surface receives negligible irradiance. The front-surface heat-balance equation is unchanged and is given by equation (1). The rear-surface heat-balance equation, a simplified form of equation (2), is

$$\frac{k}{t}(T_1 - T_2) = \epsilon_2 \sigma T_2^4 \quad (3)$$

By use of equations (1) and (3), the front- and rear-surface temperatures have been computed for a range of values of E_s , α_1 , ϵ_1 , ϵ_2 , and k/t . A rim angle θ_R of 60° was assumed for the paraboloidal mirror.

RESULTS AND DISCUSSION

Near-Earth Environment

The computed surface temperatures for paraboloidal solar concentrators have been plotted for the near-earth case in a series of figures. For each plot, table I gives the variables which are plotted as ordinate and abscissa, as well as the values of the parameters held constant. Because of the many variables, several must be held constant for each plot. Those chosen to be constant are the solar absorptances of the surfaces α_1 and α_2 and the altitude h . To see the effect of these parameters on the temperature, several plots must be compared. As indicated in table I, temperature plots are presented for values of α_1 from 0.125 to 0.2, α_2 from 0.1 to 0.9, and h from 500 kilometers to 35 000 kilometers.

Figures 2 to 6 show the computed front-surface temperature T_1 plotted against the thermal conductance of the concentrator k/t , with the front- and rear-surface emittances ϵ_1 and ϵ_2 as parameters. The front-surface emittance ϵ_1 is varied from 0.02 to 0.5 and the rear-surface emittance ϵ_2 , from 0.05 to 0.9.

The range of thermal-conductance values for each temperature plot extends from 0.01 to 1000 W/m²-°K. A concentrator of poor conductance, such as a plastic-foam structure, might be represented by a k/t value of less than 1, whereas a metal concentrator might be represented by a k/t value well above 1000. The curves are not carried beyond a k/t value of 1000 since they are nearly isothermal beyond this point.

Figures 2 to 6 indicate that the highest front-surface temperatures are experienced by a concentrator of low thermal conductance which has a front mirror surface of low emittance, such as evaporated aluminum ($\epsilon \approx 0.02$). The temperature of such a mirror may exceed 600° K on the front surface. This temperature may be greatly reduced by increasing the emittance of the front surface ϵ_1 , as by coating the reflective surface with a transparent dielectric such as silicon monoxide. The temperature of the front surface may also be reduced by constructing the concentrator of a material of good conductivity so that the rear surface may share in radiating the heat absorbed by the front surface.

The foregoing points are illustrated by figure 7, which is a crossplot of the data of figures 4 to 6 for fixed values of k/t chosen to represent a low conductance plastic-foam concentrator and a high-conductance metal concentrator. For the plastic concentrator, the front-surface temperature T_1 drops rapidly with increasing values of front-surface emittance ϵ_1 . For the metal concentrator, the temperature is not high even at low values of ϵ_1 .

Figures 8 to 12 present the computed temperature difference between the front and rear surfaces of a concentrator $T_1 - T_2$ for the same ranges of parameters used for figures 2 to 6. It is apparent from these curves that the temperature difference for a concentrator of high conductance, such as metal ($\frac{k}{t} > 1000$), is negligible, but for a concentrator of very low conductance the temperature difference may approach 500° K. This temperature difference would result in marked distortion of the concentrator. The curves also indicate that for certain combinations of parameters, the thermal gradient through the concentrator thickness can be reversed. Between these extremes, there are values of absorptance and emittance which minimize the temperature differences and limit thermal distortions arising from this source.

Equations (1) and (2) may be used to derive an expression which yields the required values of absorptance and emittance of the surfaces to satisfy the special condition that $T_1 = T_2$. Substituting T_1 for T_2 in equation (1) and solving for temperature yields

$$T_1^4 = \frac{\alpha_1 E_s}{\epsilon_1 \sigma \left(1 - \epsilon_1 \frac{\tan^2 \frac{\theta_R}{2}}{4 + \tan^2 \frac{\theta_R}{2}} \right)} \quad (4)$$

Substituting T_2 for T_1 in equation (2) and solving for temperature yields

$$T_2^4 = \frac{E_s \left(\alpha_2 a + \epsilon_2 \frac{1-a}{4} \right)}{\epsilon_2 \sigma \left(1 + \frac{h}{r_e} \right)^2} \quad (5)$$

Equating equations (4) and (5) and solving for α_2/ϵ_2 yields

$$\frac{\alpha_2}{\epsilon_2} = \frac{\frac{\alpha_1}{\epsilon_1} \left(1 + \frac{h}{r_e} \right)^2}{a \left(1 - \epsilon_1 \frac{\tan^2 \frac{\theta_R}{2}}{4 + \tan^2 \frac{\theta_R}{2}} \right)} - \frac{1-a}{4a} \quad (6)$$

Equation (6) has been used to compute the ratios of absorptance to emittance required on the front and rear surfaces to satisfy the condition that $T_1 = T_2$ when $a = 0.35$ and $\theta_R = 60^\circ$. Equation (4) has been used to compute the resulting concentrator temperature as a function of α_1/ϵ_1 . These results are shown in figure 13. Since the front- and rear-surface temperatures are equal, no heat is conducted and the thermal conductance of the concentrator is no longer a parameter. For this special case the important parameters are the ratios of solar absorptance to thermal emittance for the two surfaces, and the altitude. The absolute value of ϵ_1 does have a small effect on the curves as a result of reradiation from the concentrator front surface on to itself.

The curves of figure 13 indicate that the higher the altitude the more difficult it would be to obtain the required values of α/ϵ . At the highest altitude considered, 35 000 kilometers, it does not appear practicable to eliminate the temperature difference completely.

Solar-Probe Environment

The computed surface temperatures for paraboloidal solar concentrators for which the planetary heat contribution is negligible have been plotted in a series of figures. Table II gives the variables plotted in each figure and the values of the fixed parameters.

Figures 14 to 16 show the computed front-surface temperature plotted against the irradiance on the concentrator, expressed in solar constants, with the front- and rear-surface emittances ϵ_1 and ϵ_2 as parameters. In figure 14 temperature plots are presented for thermal conductance values k/t of 10, 100, 1000, and 10 000. Lower values of k/t were not considered for this solar-probe case because the temperatures would be unnecessarily high. Figures 15 and 16 show the front-surface temperatures for a k/t

value of 10 000, but with the front-surface solar absorptance α_1 increased to values of 0.15 and 0.20, respectively. This increase in α_1 could represent possible degradation of the mirror surface. Figures 17 to 19 show the temperature difference between the concentrator front and rear surfaces for the same conditions used for figures 14 to 16.

The curves of figures 14 to 16 indicate that a paraboloidal concentrator, used as part of a solar probe, may reach high temperatures even if high emittance coatings are employed. A rear surface of high emittance tends to decrease the front-surface temperature by increasing the heat conducted from front to back but, as shown by figures 17 to 19, this condition also increases the temperature difference between the surfaces and thus tends to produce more distortion of the paraboloid. These effects may more easily be seen in the crossplots presented as figures 20 and 21, which illustrate the effects of varying the surface emittances on the surface temperatures for a concentrator of low conductivity ($\frac{k}{t} = 10 \frac{W}{m^2 \cdot ^\circ K}$) and one of high conductivity ($\frac{k}{t} = 10\,000 \frac{W}{m^2 \cdot ^\circ K}$) when subjected to a solar irradiance of 20 solar constants. Figure 20 indicates that the front-surface temperature T_1 may be reduced several hundred degrees with the application of high emittance coatings, but the lowest temperature computed is still in excess of $450^\circ K$. Figure 21 indicates that the distortion-causing temperature difference $T_1 - T_2$ will be increased by the use of a high emittance coating, such as paint, on the rear surface. However, this temperature difference is drastically reduced by an increase in conductance from $k/t = 10$ to $k/t = 10\,000$. A metal concentrator would probably exceed a conductance of $\frac{k}{t} = 10\,000 \frac{W}{m^2 \cdot ^\circ K}$. Such a metal concentrator, as well as having reduced distortion from this thermal gradient, would be better able to withstand the high temperature at which a solar probe must operate.

CONCLUDING REMARKS

Steady-state equations have been developed which yield the front- and rear-surface temperatures of a paraboloidal mirror in space aimed at the sun. These equations have been solved and the temperatures plotted for a range of the important parameters.

The results indicate that at an irradiance of one solar constant, a concentrator with very low thermal conductance may exceed a temperature of $600^\circ K$ in space, unless a front-surface coating is used to increase the emittance. The temperature difference between the front and rear surface, which causes thermal distortion of the mirror, may be greatly reduced by proper selection of thermal control coatings if the concentrator is near the earth. At irradiances of many solar constants, as in the case of a solar probe,

high emittance surfaces and metal construction appear to be needed to reduce the front-surface temperature and to minimize thermal distortion.

Langley Research Center,

National Aeronautics and Space Administration,

Langley Station, Hampton, Va., February 10, 1969,

120-33-06-08-23.

APPENDIX A

DERIVATION OF EXPRESSION FOR E_m

The front surface of the paraboloidal mirror radiates heat due to its own temperature, part of which is intercepted by its own surface. The irradiance on an elementary area dA at the center of the front surface from this source is (fig. 22)

$$E_m = \frac{\epsilon_1 \sigma T_1^4 A_1 F_{A_1 \rightarrow dA}}{dA} \quad (A1)$$

where T_1 is assumed to be constant over the front surface and $F_{A_1 \rightarrow dA}$ is the configuration factor, defined as the fraction of the radiation from surface 1 which is incident on dA by direct radiation. Additional radiation which may reach dA by subsequent reflection from surface 1 is neglected.

From the reciprocity relation,

$$A_1 F_{A_1 \rightarrow dA} = dA F_{dA \rightarrow A_1} \quad (A2)$$

where A_1 is the area of the front surface of the concentrator and $F_{dA \rightarrow A_1}$ represents the fraction of the radiation leaving the front surface of dA which is incident on surface 1.

The configuration factor for diffuse radiation from an elementary area to a directly opposite parallel disk is derived in reference 5 and may be written as

$$F_{dA \rightarrow D_R} = \sin^2 \beta_R \quad (A3)$$

In this case the disk is that plane area enclosed by the rim of the paraboloid. (See fig. 22.) Since $F_{dA \rightarrow A_1} + F_{dA \rightarrow D_R} = 1$,

$$F_{dA \rightarrow A_1} = 1 - \sin^2 \beta_R \quad (A4)$$

Substituting equation (A4) into equation (A2) yields

$$A_1 F_{A_1 \rightarrow dA} = dA \left(1 - \sin^2 \beta_R \right) \quad (A5)$$

If surface 1 is a paraboloid, $\sin^2 \beta_R$ may be expressed in terms of rim angle θ_R as

$$\sin^2 \beta_R = \frac{1}{1 + \frac{1}{4} \tan^2 \frac{\theta_R}{2}} \quad (A6)$$

APPENDIX A

Substituting equations (A5) and (A6) into equation (A1) yields

$$E_m = \epsilon_1 \sigma T_1^4 \left(\frac{\tan^2 \frac{\theta_R}{2}}{4 + \tan^2 \frac{\theta_R}{2}} \right)$$

APPENDIX B

DERIVATION OF EXPRESSION FOR E_e

The earth absorbs, on the average, about 65 percent of the incident solar energy and reemits this energy as thermal radiation. Since the emitting area of the earth is four times that of its projected area, the energy emitted per unit surface area of the earth per unit time is, on the average, $\frac{E_s(1-a)}{4}$.

For the case of diffuse radiation between a sphere and an elementary area, the sphere may be thought of as replaced by a diffuse disk which radiates equal power per unit surface area, and which appears to have the same boundary when viewed from the elementary area. (See ref. 6 and fig. 23.) The irradiance on the rear surface of the elementary area dA due to this emitted energy is then

$$E_e = \frac{E_s(1-a)\pi r_d^2 F_{D_e \rightarrow dA}}{4dA} \quad (B1)$$

where r_d is the radius of the substitute disk and $F_{D_e \rightarrow dA}$ is the configuration factor from the disk to dA .

From the reciprocity relation and equation (B1),

$$E_e = \frac{E_s(1-a)}{4} F_{dA \rightarrow D_e} \quad (B2)$$

where the configuration factor $F_{dA \rightarrow D_e}$ represents the fraction of the emitted energy from dA which is incident on the disk. It may be expressed as

$$F_{dA \rightarrow D_e} = \sin^2 \varphi = \frac{r_e^2}{(r_e + h)^2} = \frac{1}{\left(1 + \frac{h}{r_e}\right)^2} \quad (B3)$$

Substituting equation (B3) into equation (B2) yields

$$E_e = \frac{E_s(1-a)}{4 \left(1 + \frac{h}{r_e}\right)^2}$$

APPENDIX C

DERIVATION OF EXPRESSION FOR E_a

As for most thermal balance calculations for satellites, the earth is assumed to have a diffuse surface which reflects 35 percent of the incident solar radiation without changing its spectral distribution. To simplify the calculation of E_a further, it is assumed that the earth may be replaced by a diffuse disk which appears to have the same boundary when viewed from dA (see fig. 23) and is of the same reflectance. This assumption introduces an error because the disk is uniformly irradiated by the sun but the earth is not. The magnitude of this error is discussed later.

The irradiance on the rear surface of the elementary area dA due to reflected energy from the diffuse disk is

$$E_a = \frac{E_s \pi r_d^2 a F_{D_e \rightarrow dA}}{dA} \quad (C1)$$

where r_d is the radius of the disk and $F_{D_e \rightarrow dA}$ is the configuration factor, defined as the fraction of the radiation leaving the disk which is incident on dA . From the reciprocity relation and equation (C1),

$$E_a = E_s a F_{dA \rightarrow D_e} \quad (C2)$$

where $F_{dA \rightarrow D_e}$ is the configuration factor from dA to the disk. An expression for this configuration factor is

$$F_{dA \rightarrow D_e} = \sin^2 \varphi = \frac{r_e^2}{(r_e + h)^2} = \frac{1}{\left(1 + \frac{h}{r_e}\right)^2} \quad (C3)$$

Substituting equation (C3) into equation (C2) yields

$$E_a = \frac{E_s a}{\left(1 + \frac{h}{r_e}\right)^2}$$

This expression overestimates the irradiance on the concentrator because the assumed diffuse disk is uniformly irradiated by the sun but the earth's surface is not. The error in albedo irradiance of the concentrator appears to be negligible at low altitudes but would approach 50 percent at extreme altitudes. At the highest altitude considered herein (35 000 kilometers), the error is estimated at 33 percent. This error would have little effect on the temperature of a concentrator of good conductance since

APPENDIX C

the albedo contribution at high altitudes is small compared with that of the direct sun, but for a concentrator of very poor conductance, this overestimation could result in a calculated temperature which is too high by as much as 15° K on the rear surface.

REFERENCES

1. Heath, Atwood R., Jr.; and Hoffman, Edward L.: Recent Gains in Solar Concentrator Technology. *J. Spacecraft Rockets*, vol. 4, no. 5, May 1967, pp. 621-624.
2. Walz, Joseph E.: *Thermal Distortions of Thin-Walled Paraboloidal Shells*. NASA TN D-3543, 1966.
3. Thompson Ramo Wooldridge, Inc.: *60-Inch Stretch-Formed Aluminum Solar Concentrator*. NASA CR-47, 1964.
4. Thomas, Ronald L.: *Analog Computer Study of Temperature Gradients of a Solar Collector in Ecliptic Earth Orbit*. NASA TM X-1282, 1966.
5. Gebhart, Benjamin: *Heat Transfer*. McGraw-Hill Book Co., Inc., c.1961.
6. Walsh, John W. T.: *Photometry*. Third ed., Dover Publ., Inc., c.1958.

TABLE I.- LIST OF FIGURES FOR NEAR-EARTH CASE

Figure	Ordinate	Abscissa	Values of constant parameters		
			α_1	α_2	h, km
2(a)	T_1	k/t	0.125	0.1	500
2(b)	T_1	k/t	.125	.1	5 000
2(c)	T_1	k/t	.125	.1	35 000
3(a)	T_1	k/t	.125	.5	500
3(b)	T_1	k/t	.125	.5	5 000
3(c)	T_1	k/t	.125	.5	35 000
4(a)	T_1	k/t	.125	.9	500
4(b)	T_1	k/t	.125	.9	5 000
4(c)	T_1	k/t	.125	.9	35 000
5(a)	T_1	k/t	.15	.9	500
5(b)	T_1	k/t	.15	.9	5 000
5(c)	T_1	k/t	.15	.9	35 000
6(a)	T_1	k/t	.20	.9	500
6(b)	T_1	k/t	.20	.9	5 000
6(c)	T_1	k/t	.20	.9	35 000
7	T_1	ϵ_1	Various	.9	500
8(a)	$T_1 - T_2$	k/t	.125	.1	500
8(b)	$T_1 - T_2$	k/t	.125	.1	5 000
8(c)	$T_1 - T_2$	k/t	.125	.1	35 000
9(a)	$T_1 - T_2$	k/t	.125	.5	500
9(b)	$T_1 - T_2$	k/t	.125	.5	5 000
9(c)	$T_1 - T_2$	k/t	.125	.5	35 000
10(a)	$T_1 - T_2$	k/t	.125	.9	500
10(b)	$T_1 - T_2$	k/t	.125	.9	5 000
10(c)	$T_1 - T_2$	k/t	.125	.9	35 000
11(a)	$T_1 - T_2$	k/t	.15	.9	500
11(b)	$T_1 - T_2$	k/t	.15	.9	5 000
11(c)	$T_1 - T_2$	k/t	.15	.9	35 000
12(a)	$T_1 - T_2$	k/t	.20	.9	500
12(b)	$T_1 - T_2$	k/t	.20	.9	5 000
12(c)	$T_1 - T_2$	k/t	.20	.9	35 000
13	α_2/ϵ_2	α_1/ϵ_1	-----	--	-----

TABLE II.- LIST OF FIGURES FOR SOLAR-PROBE CASE

Figure	Ordinate	Abscissa	Values of parameters	
			α_1	$k/t, \frac{W}{m^2 \cdot ^\circ K}$
14(a)	T_1	Solar constant	0.125	10
14(b)	T_1	Solar constant	.125	100
14(c)	T_1	Solar constant	.125	1 000
14(d)	T_1	Solar constant	.125	10 000
15	T_1	Solar constant	.15	10 000
16	T_1	Solar constant	.20	10 000
17(a)	$T_1 - T_2$	Solar constant	.125	10
17(b)	$T_1 - T_2$	Solar constant	.125	100
17(c)	$T_1 - T_2$	Solar constant	.125	1 000
17(d)	$T_1 - T_2$	Solar constant	.125	10 000
18	$T_1 - T_2$	Solar constant	.15	10 000
19	$T_1 - T_2$	Solar constant	.20	10 000
20	T_1	ϵ_1	.125	10 and 10 000
21	$T_1 - T_2$	ϵ_1	.125	10 and 10 000

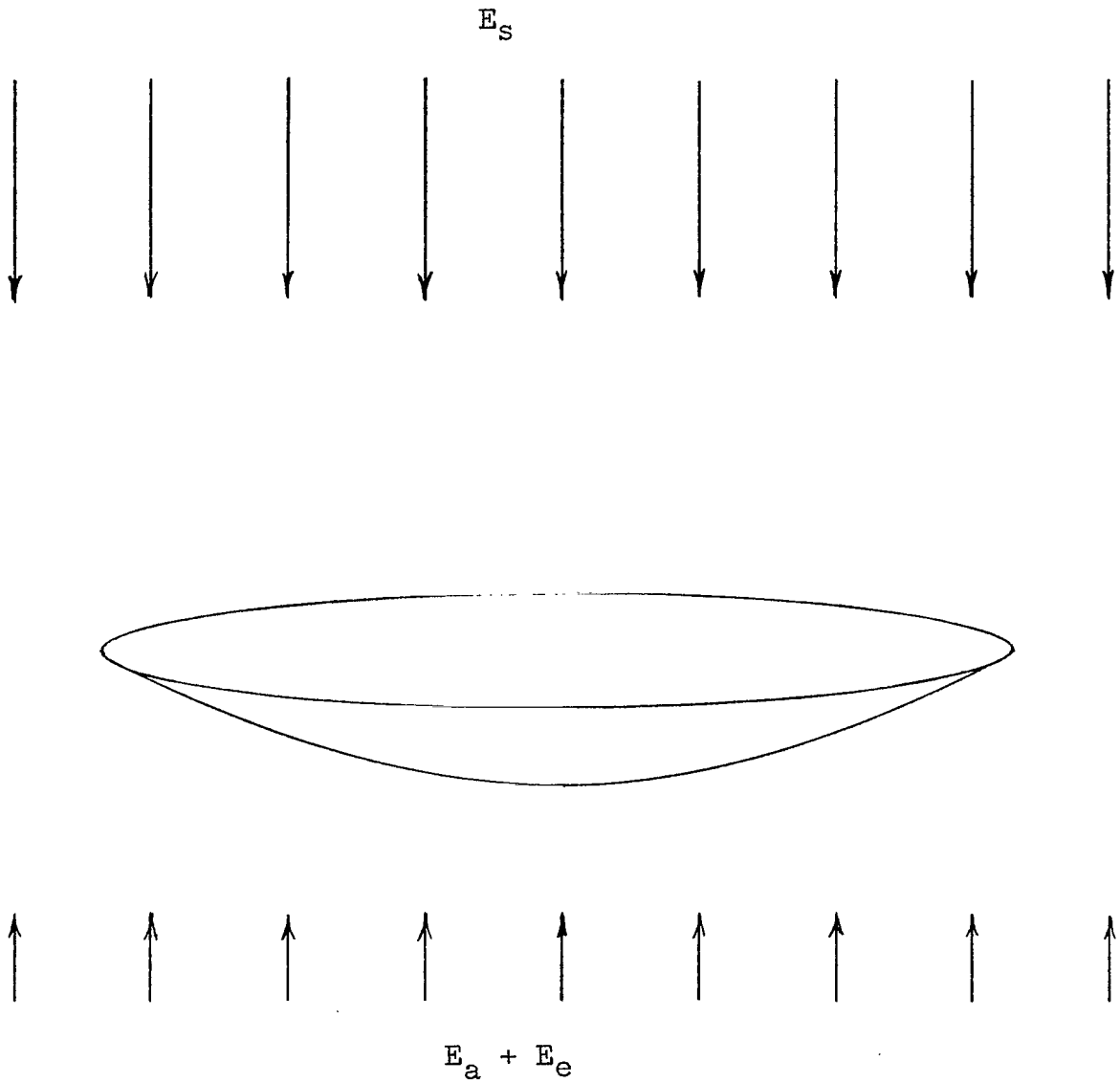
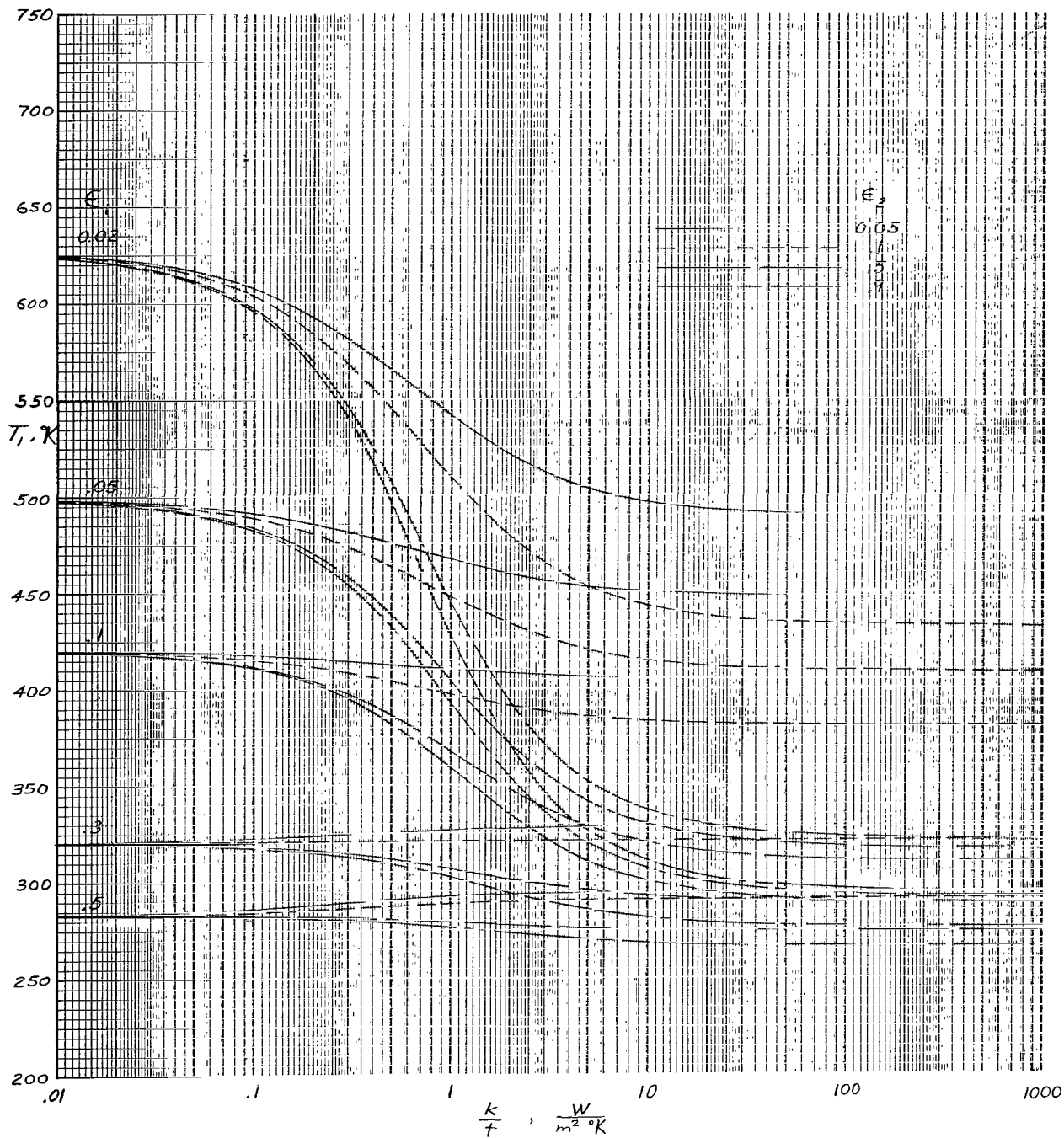
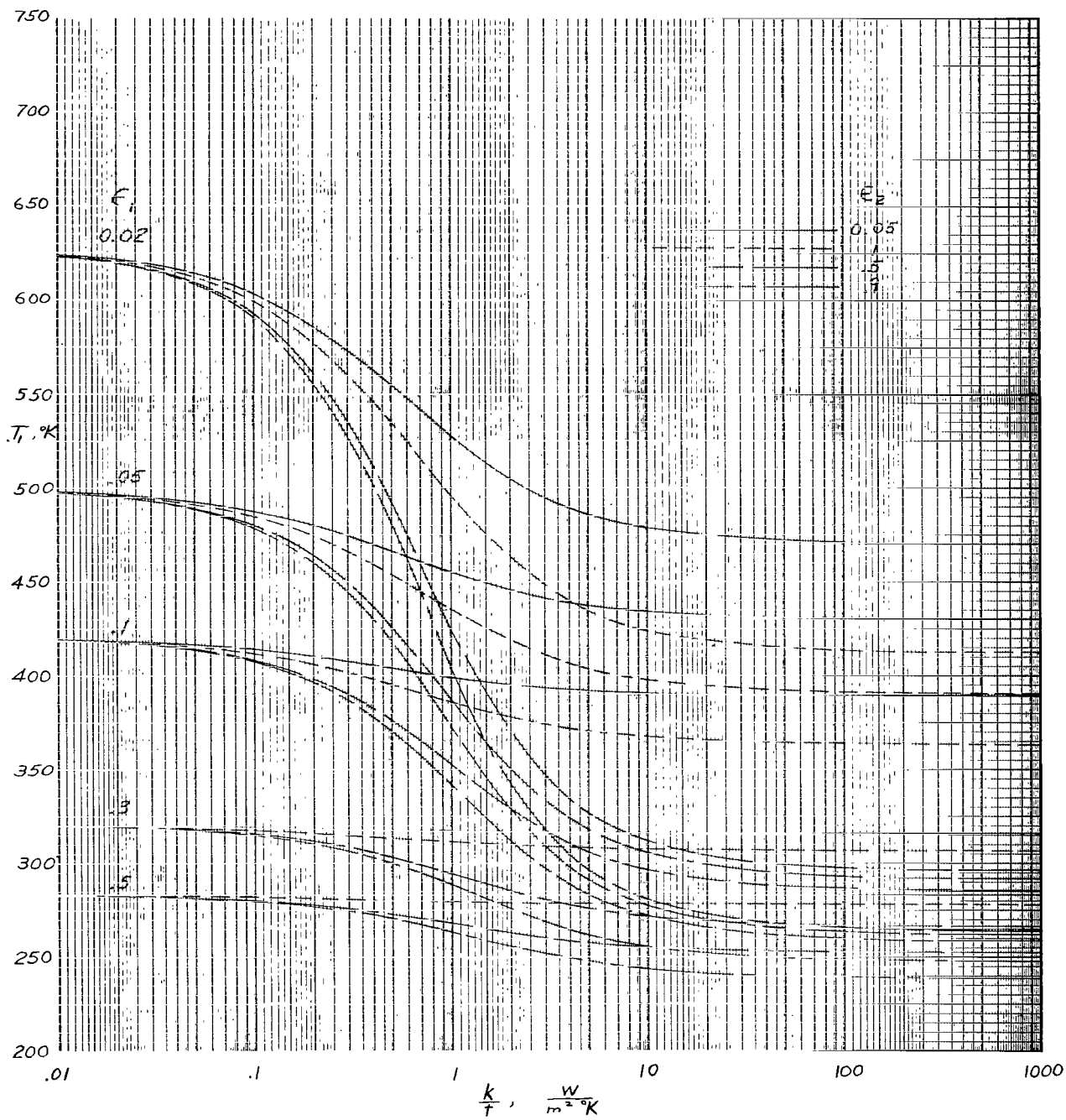


Figure 1.- Schematic of paraboloidal mirror with heat inputs from sun and earth.



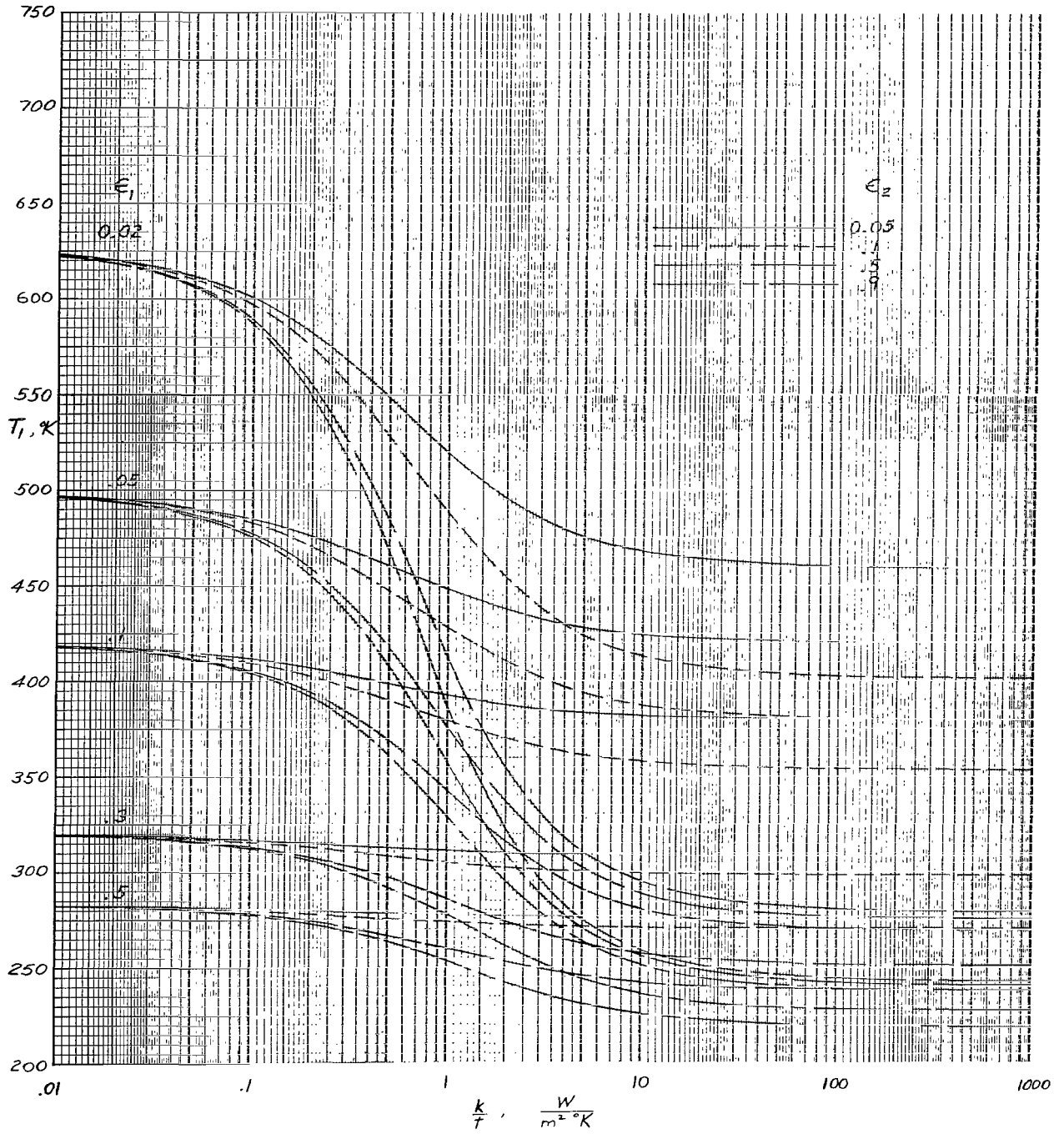
(a) $h = 500$ km.

Figure 2.- Front-surface temperature of paraboloidal mirror for near-earth case. $\alpha_1 = 0.125$; $\alpha_2 = 0.1$; $\theta_R = 60^\circ$.



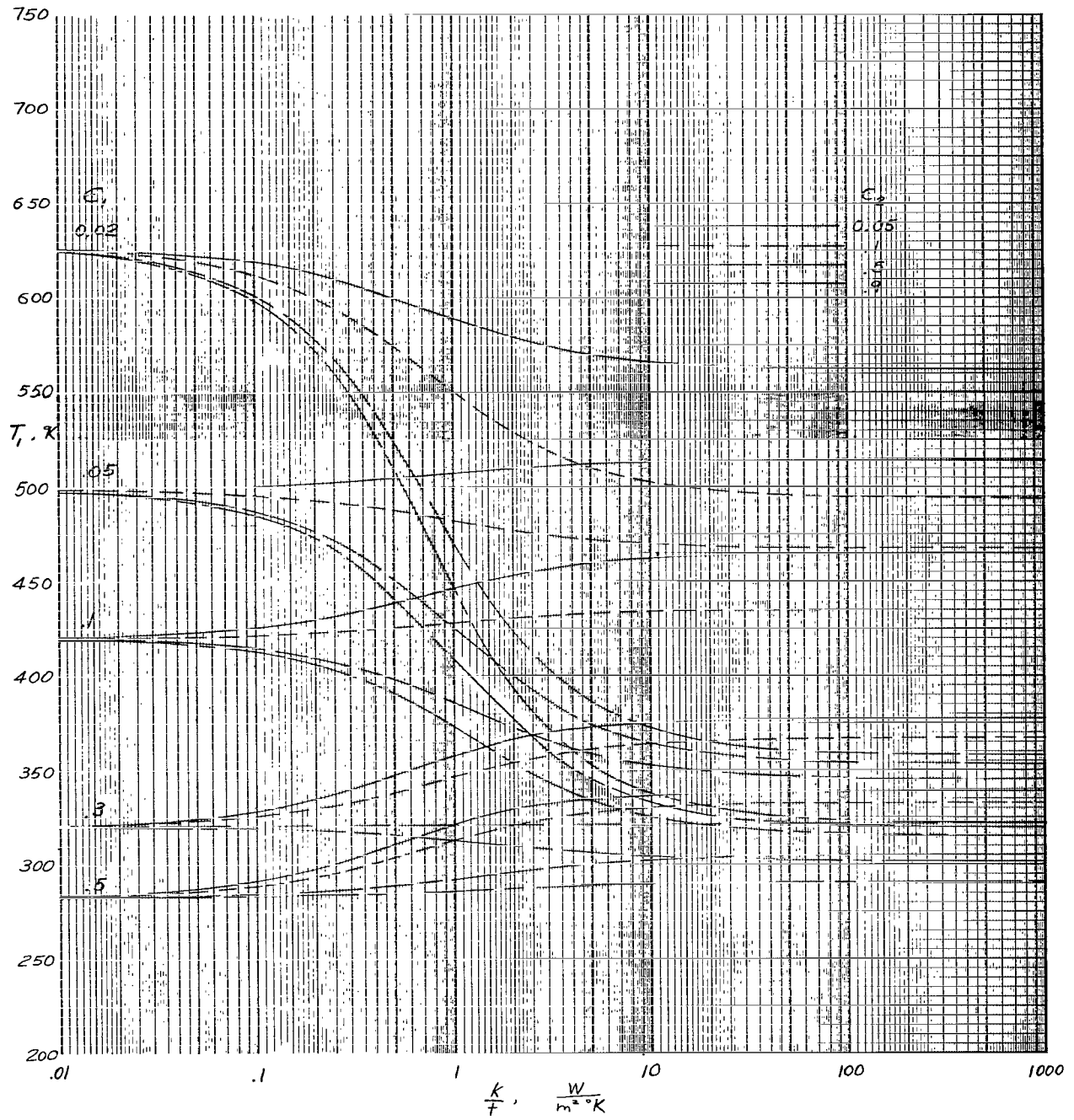
(b) $h = 5000$ km.

Figure 2.- Continued.



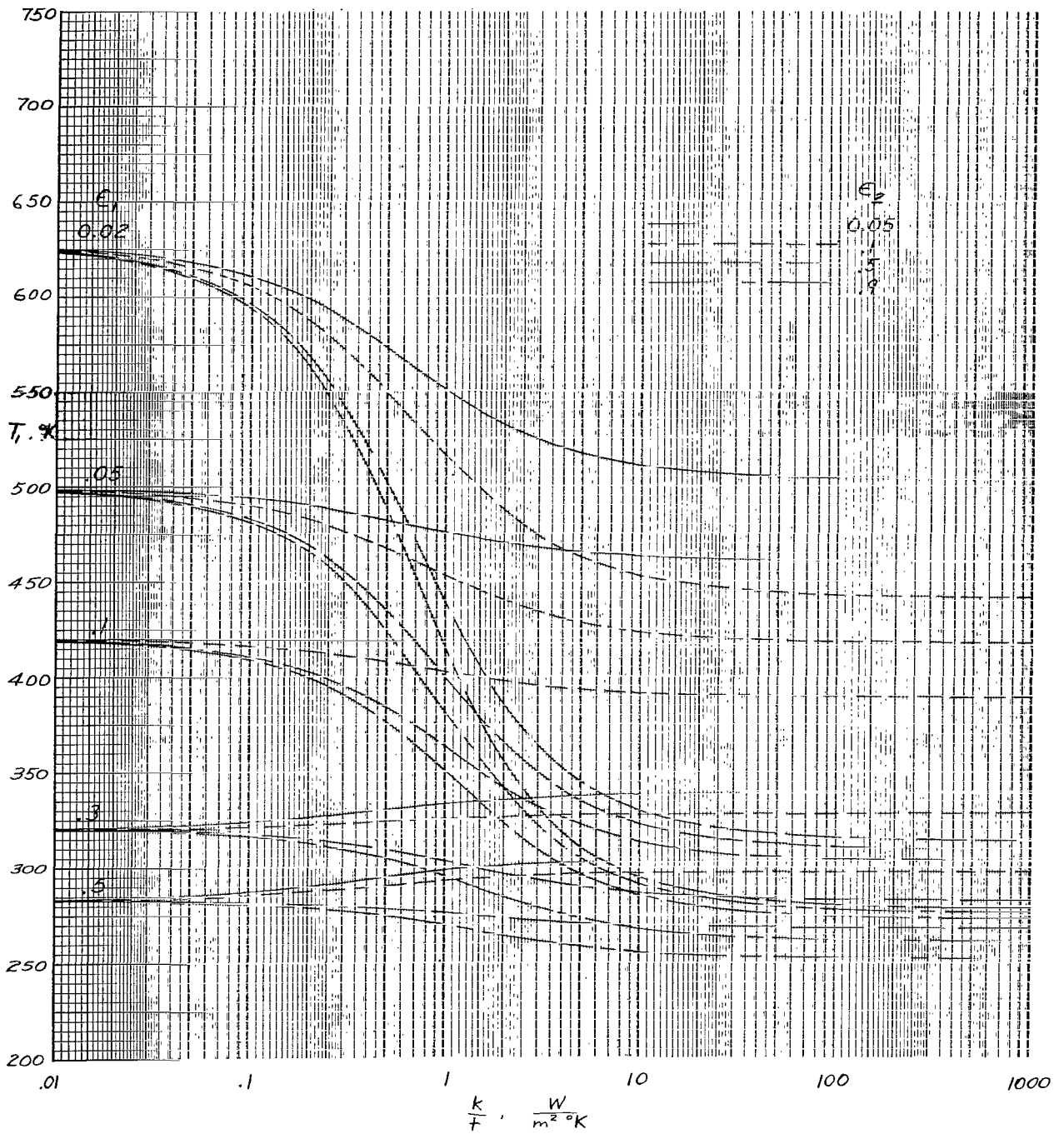
(c) $h = 35\ 000\ km.$

Figure 2.- Concluded.



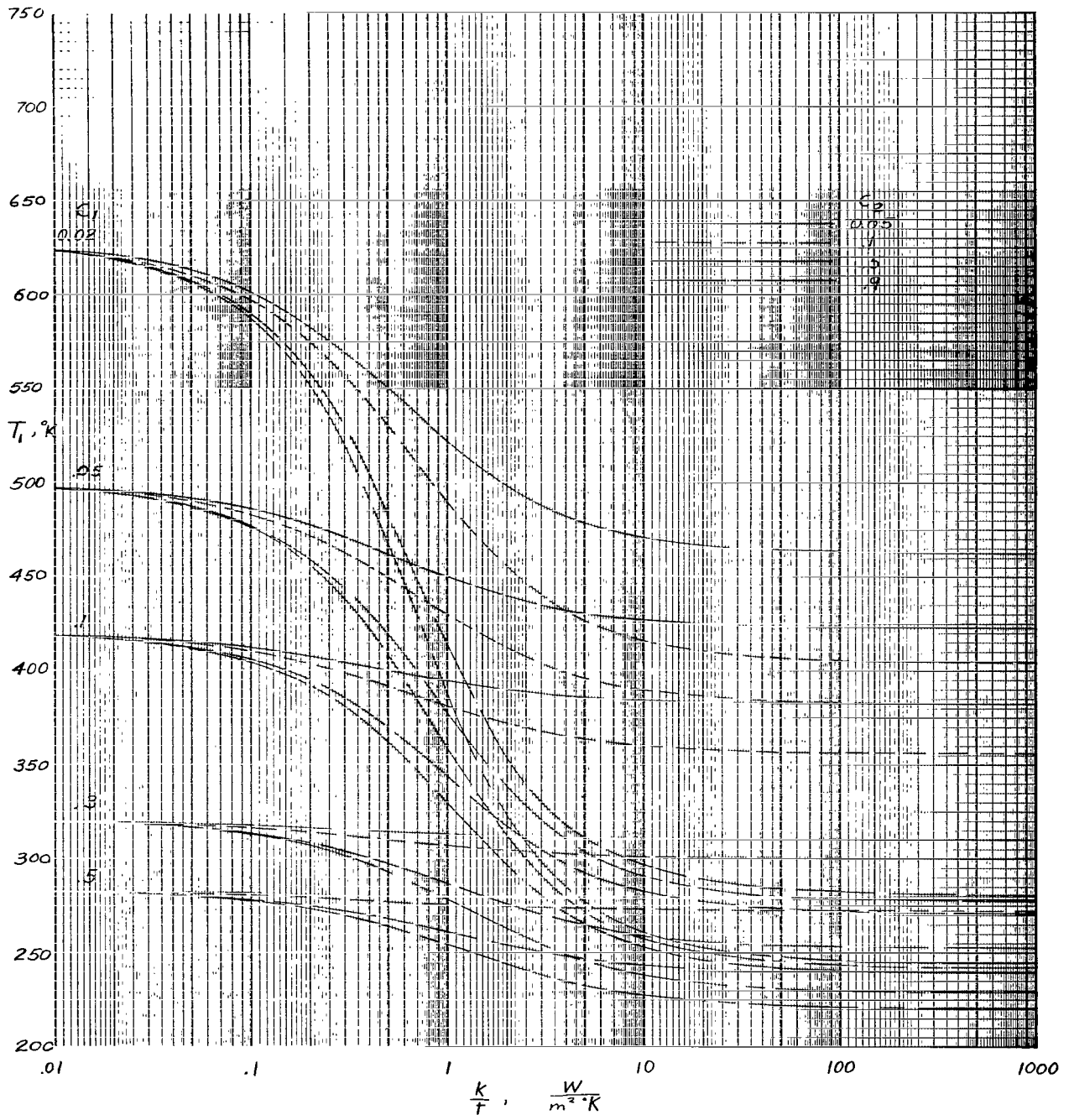
(a) $h = 500$ km.

Figure 3.- Front-surface temperature of paraboloidal mirror for near-earth case. $\alpha_1 = 0.125$; $\alpha_2 = 0.5$; $\theta_R = 60^\circ$.



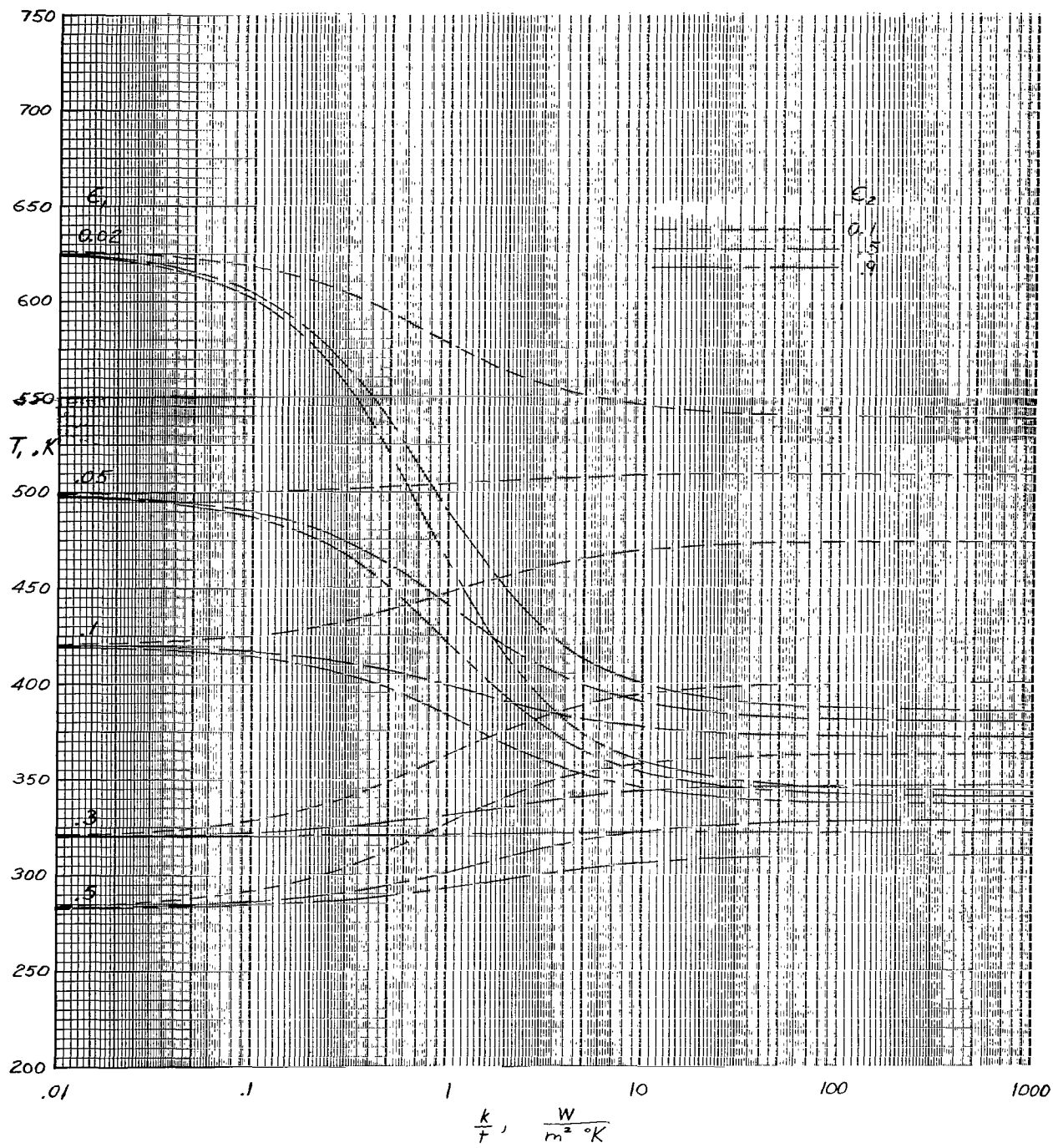
(b) $h = 5000$ km.

Figure 3.- Continued.



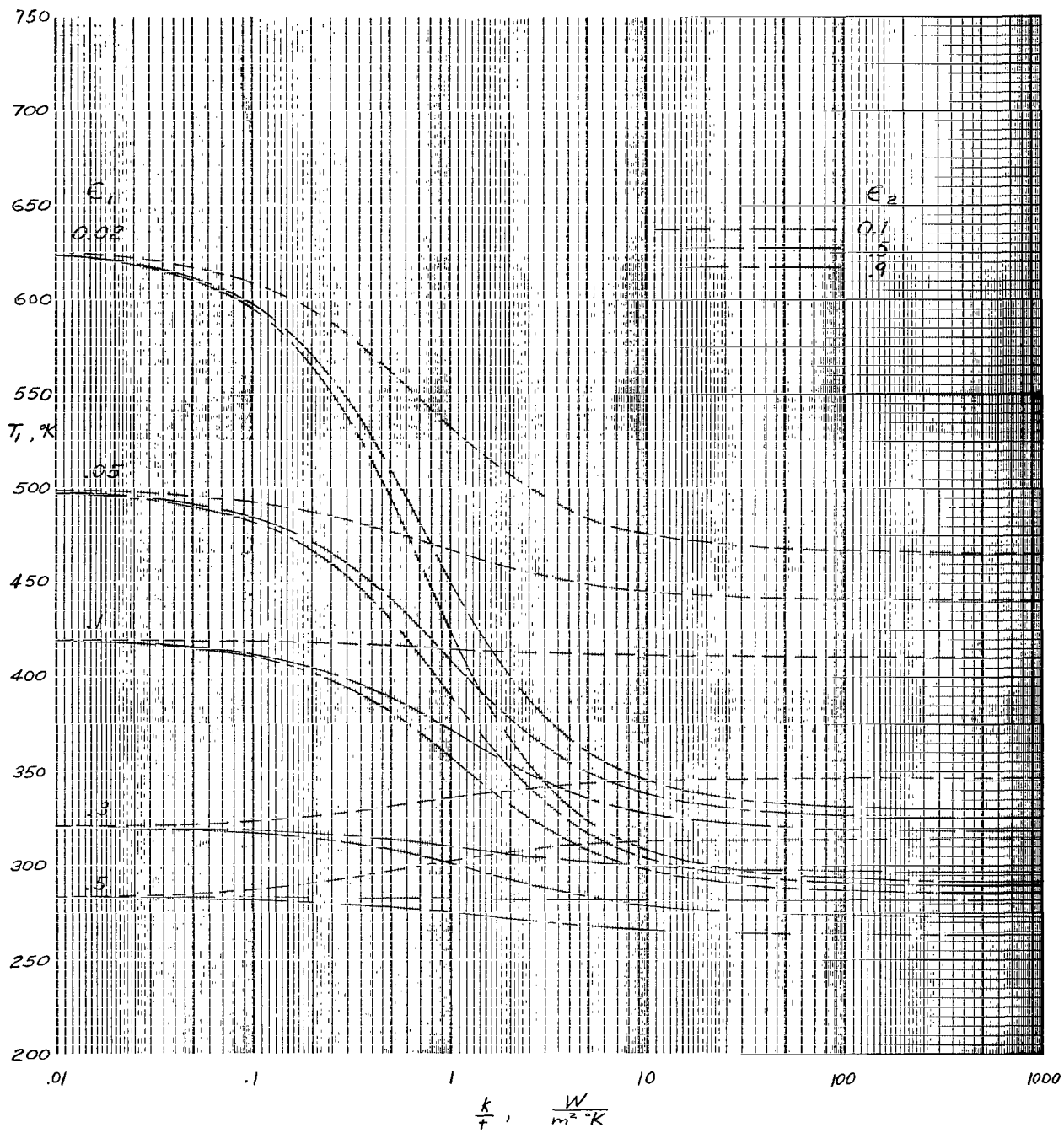
(c) $h = 35\,000$ km.

Figure 3.- Concluded.



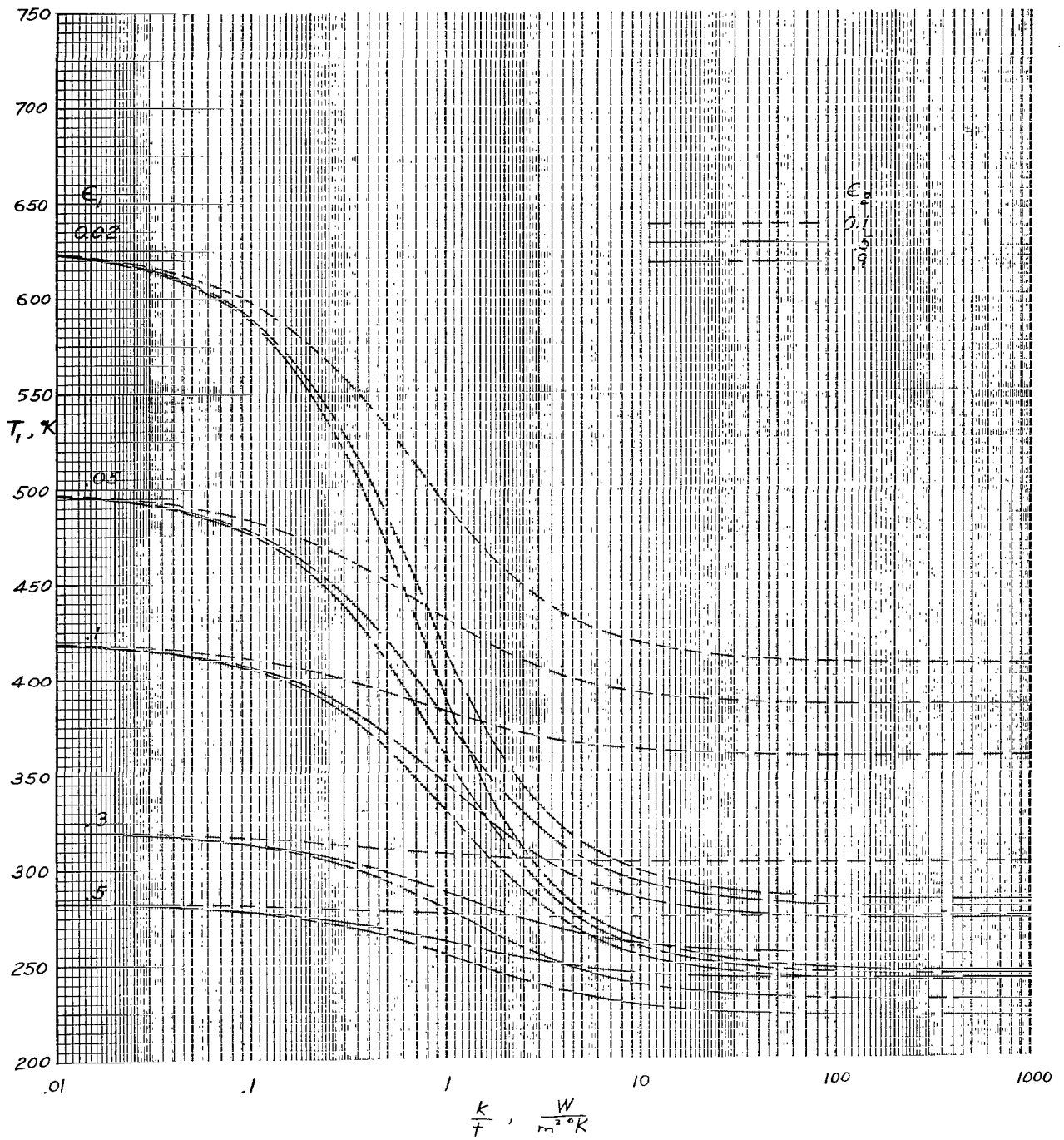
(a) $h = 500$ km.

Figure 4.- Front-surface temperature of paraboloidal mirror for near-earth case. $\alpha_1 = 0.125$; $\alpha_2 = 0.9$; $\theta_R = 60^\circ$.



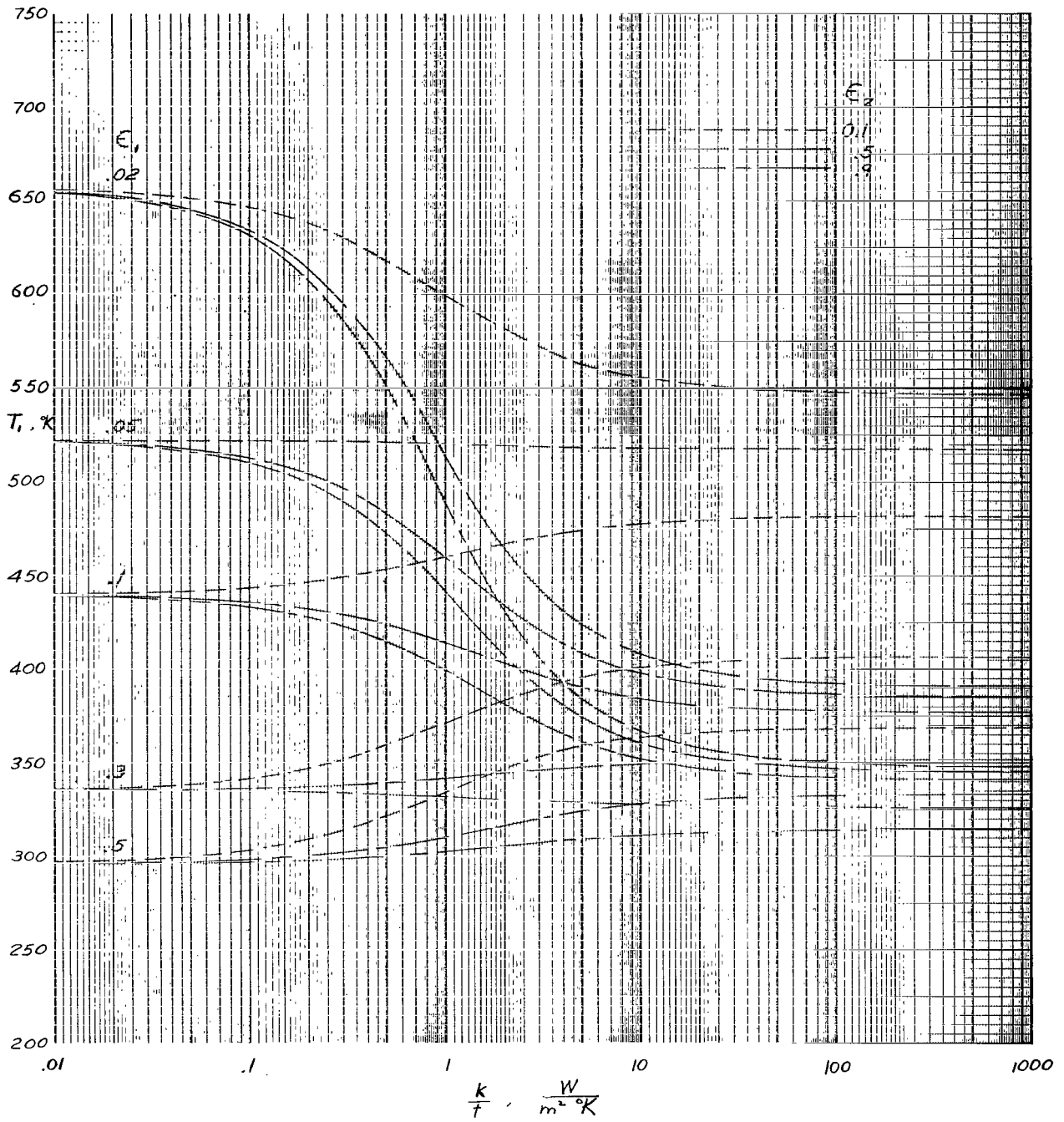
(b) $h = 5000 \text{ km.}$

Figure 4.- Continued.



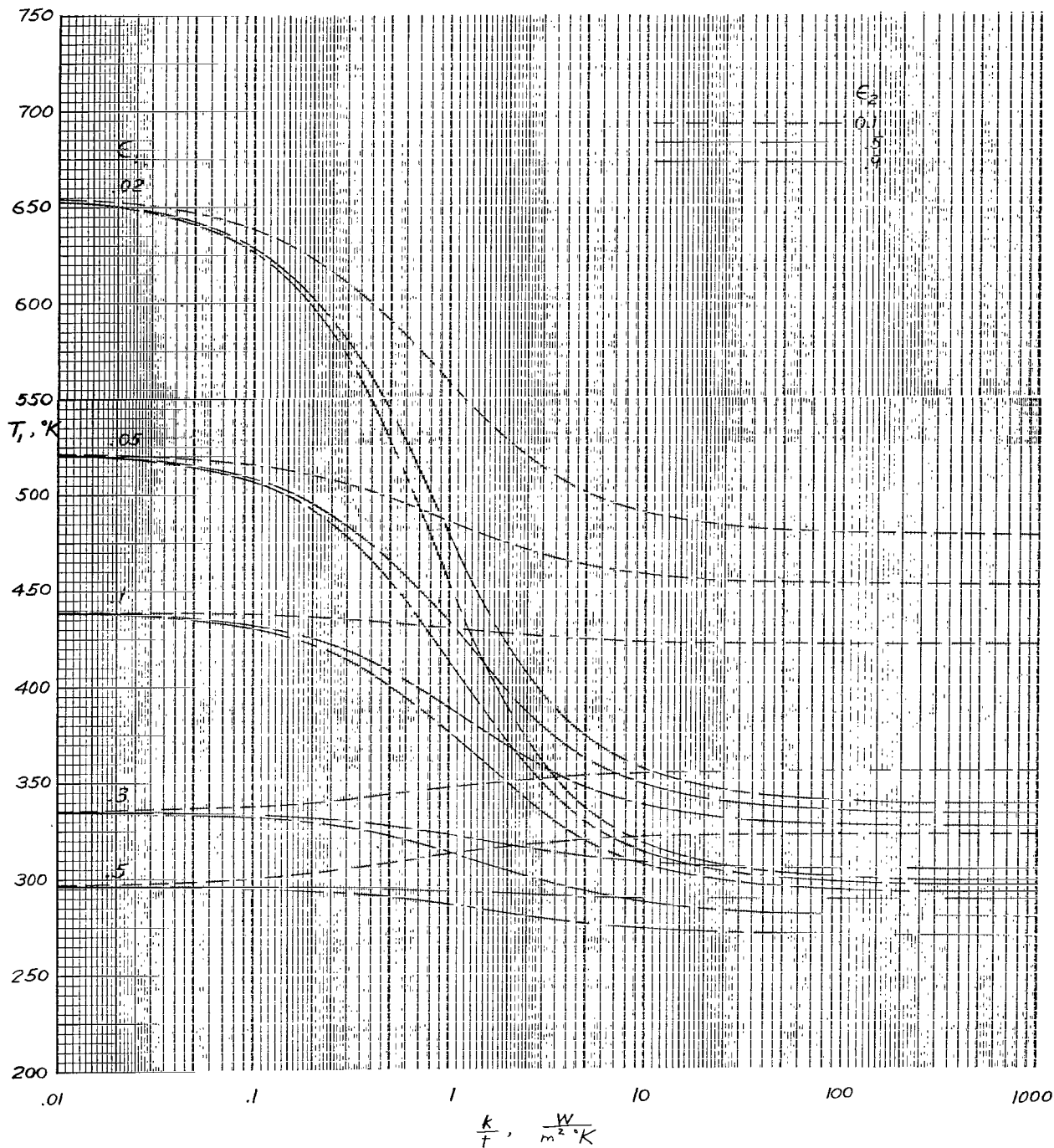
(c) $h = 35\,000$ km.

Figure 4.- Concluded.



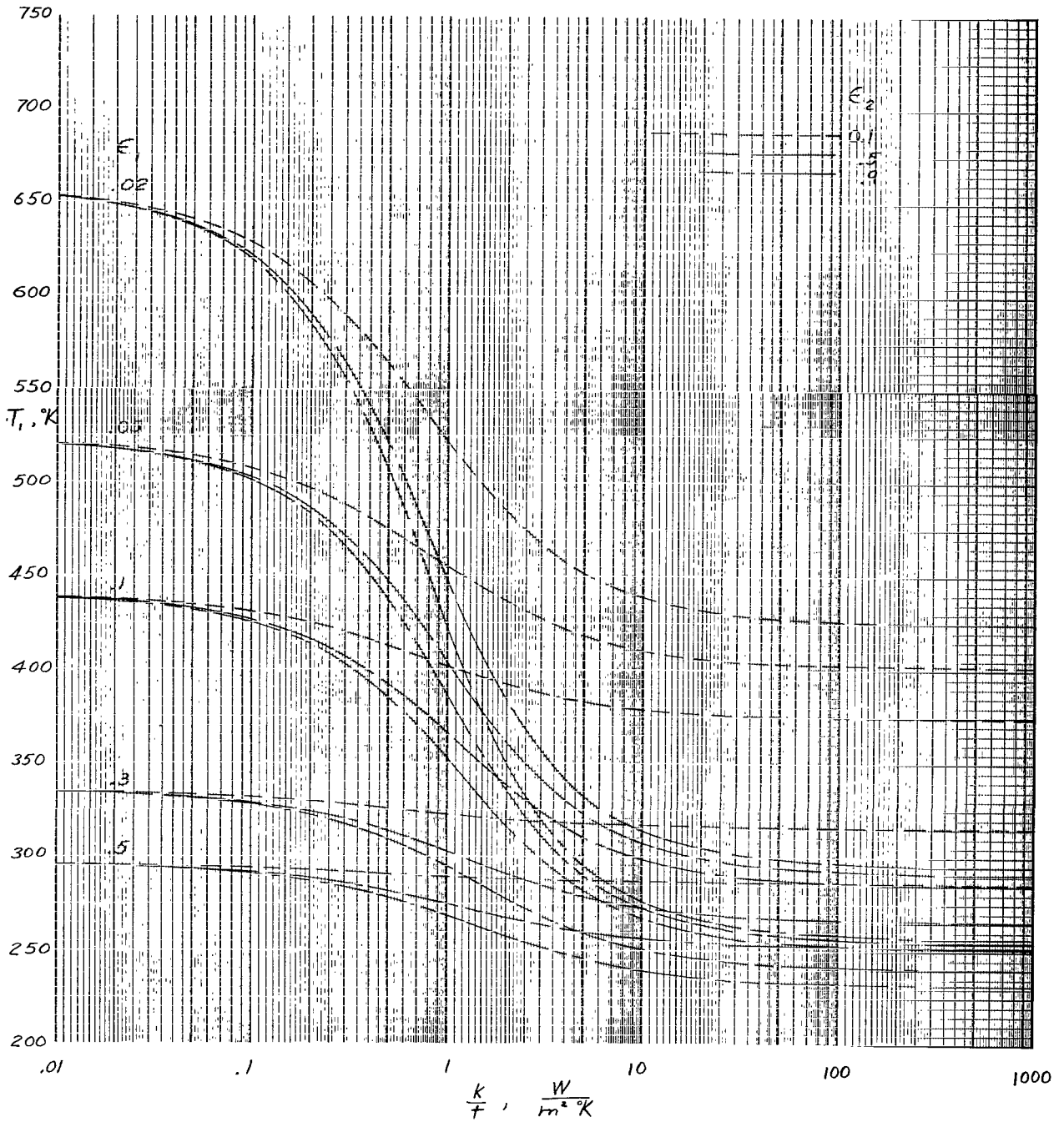
(a) $h = 500$ km.

Figure 5.- Front-surface temperature of paraboloidal mirror for near-earth case. $\alpha_1 = 0.15$; $\alpha_2 = 0.9$; $\theta_R = 60^\circ$.



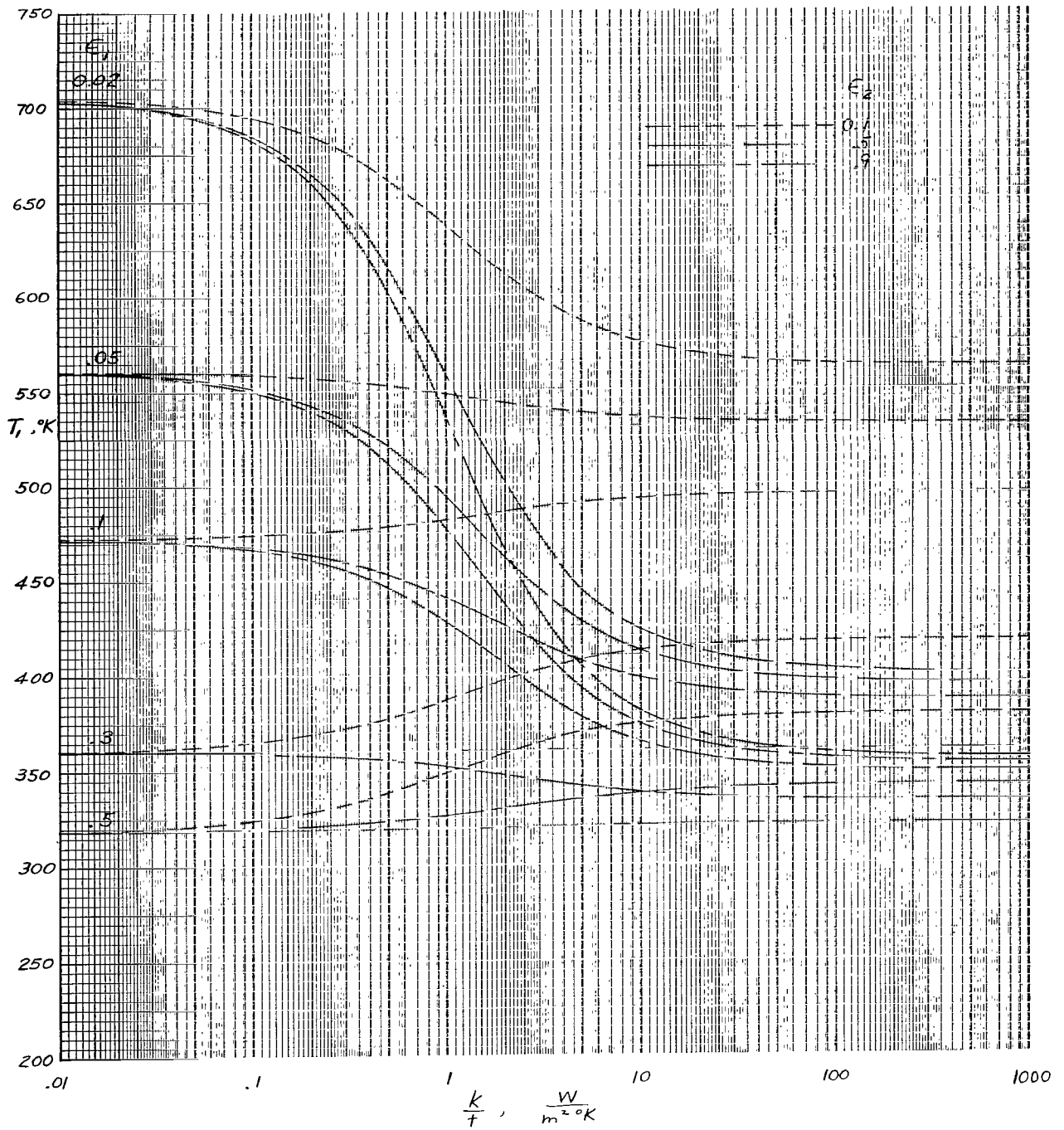
(b) $h = 5000$ km.

Figure 5.- Continued.



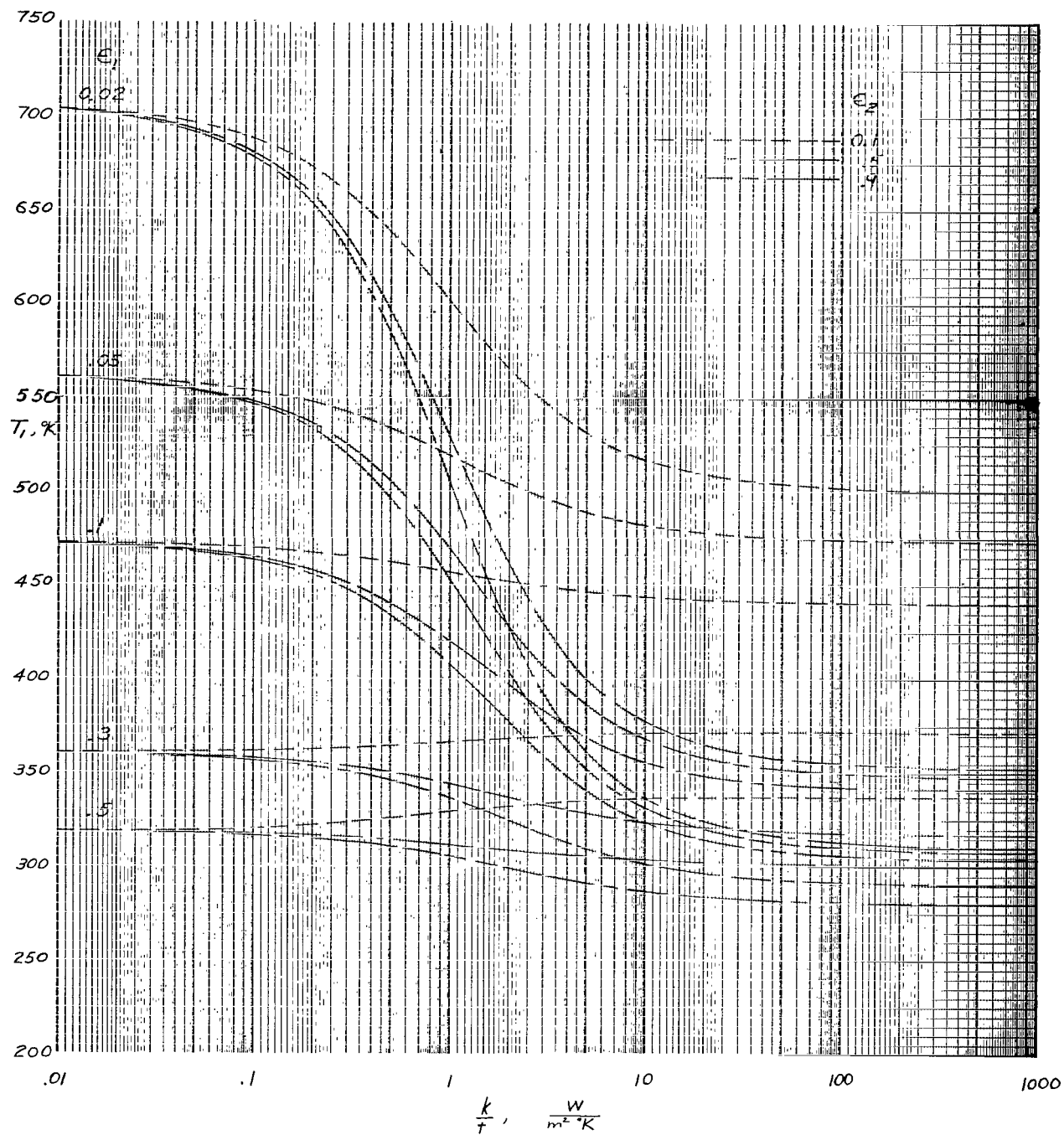
(c) $h = 35\ 000$ km.

Figure 5.- Concluded.



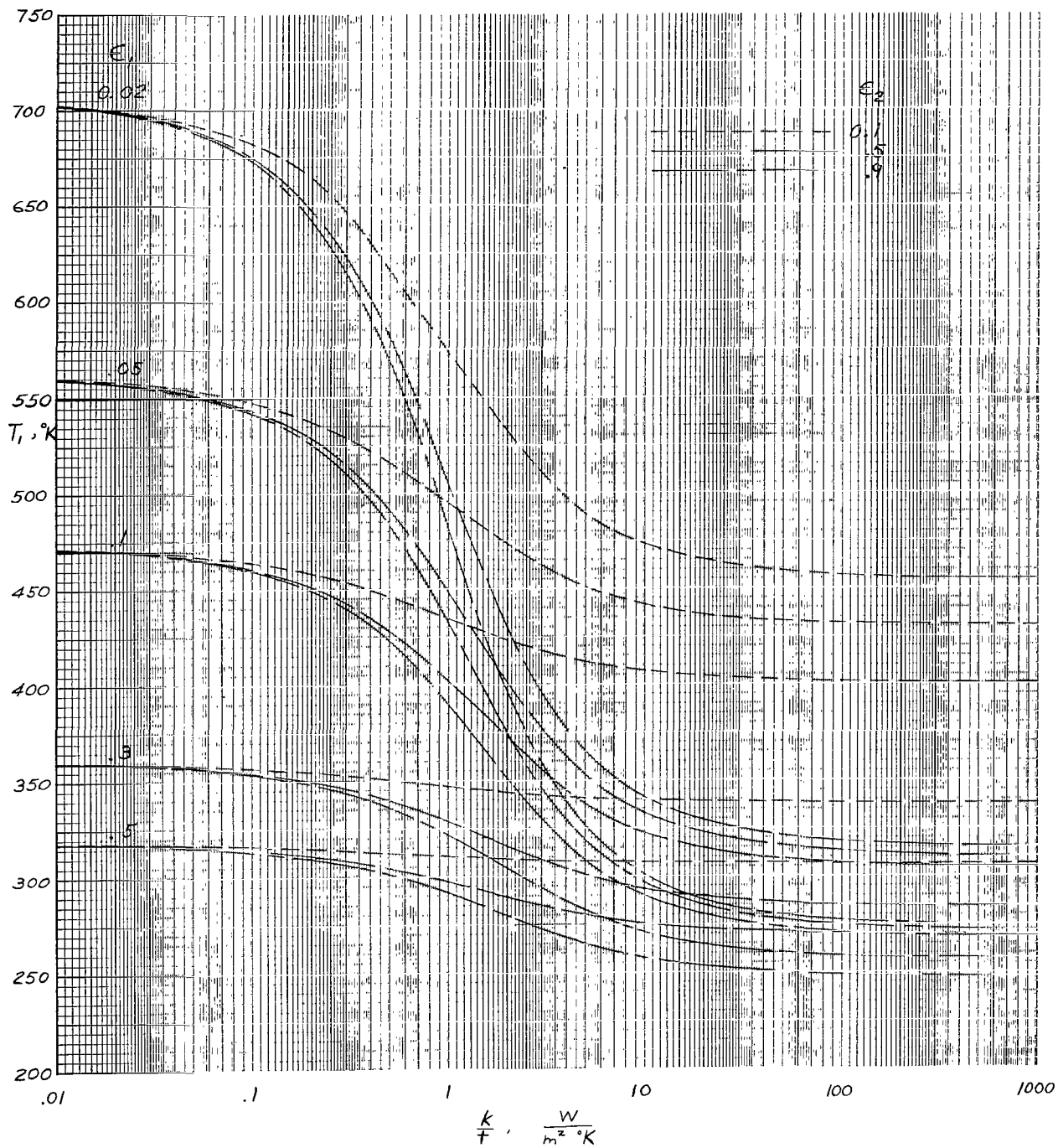
(a) $h = 500$ km.

Figure 6.- Front-surface temperature of paraboloidal mirror for near-earth case. $\alpha_1 = 0.2$; $\alpha_2 = 0.9$; $\theta_R = 60^\circ$.



(b) $h = 5000$ km.

Figure 6.- Continued.



(c) $h = 35\ 000\ km.$

Figure 6.- Concluded.

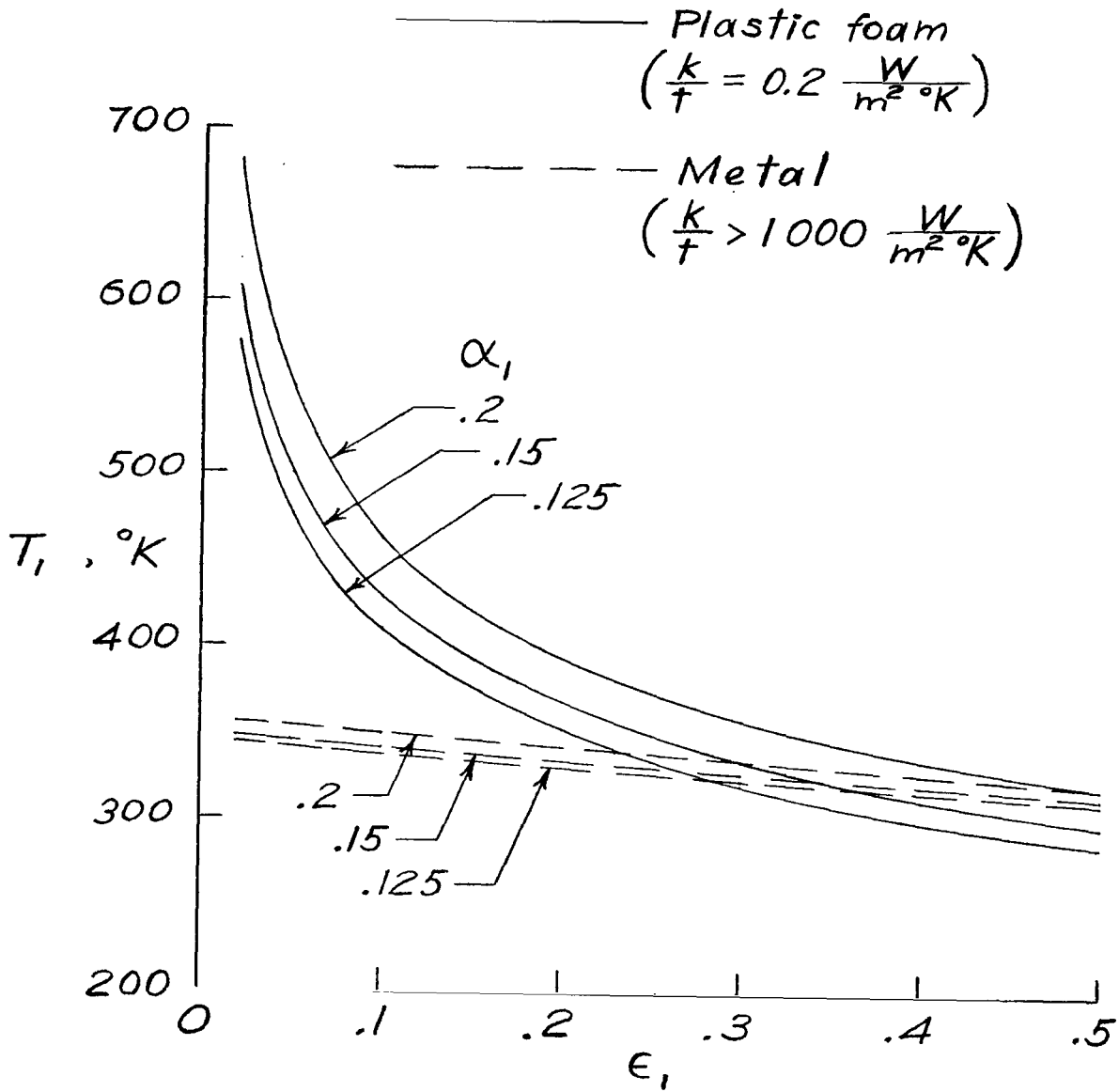
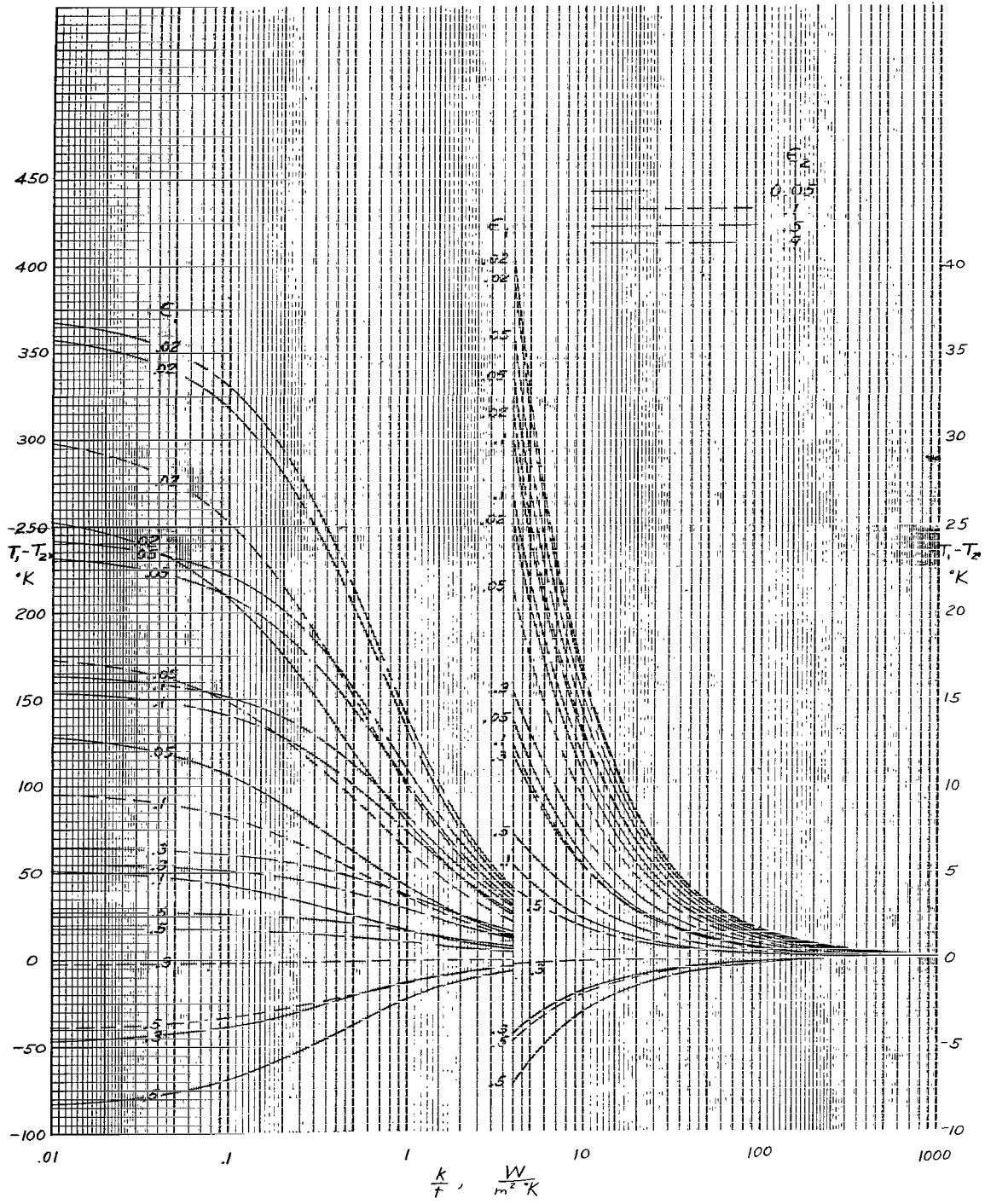
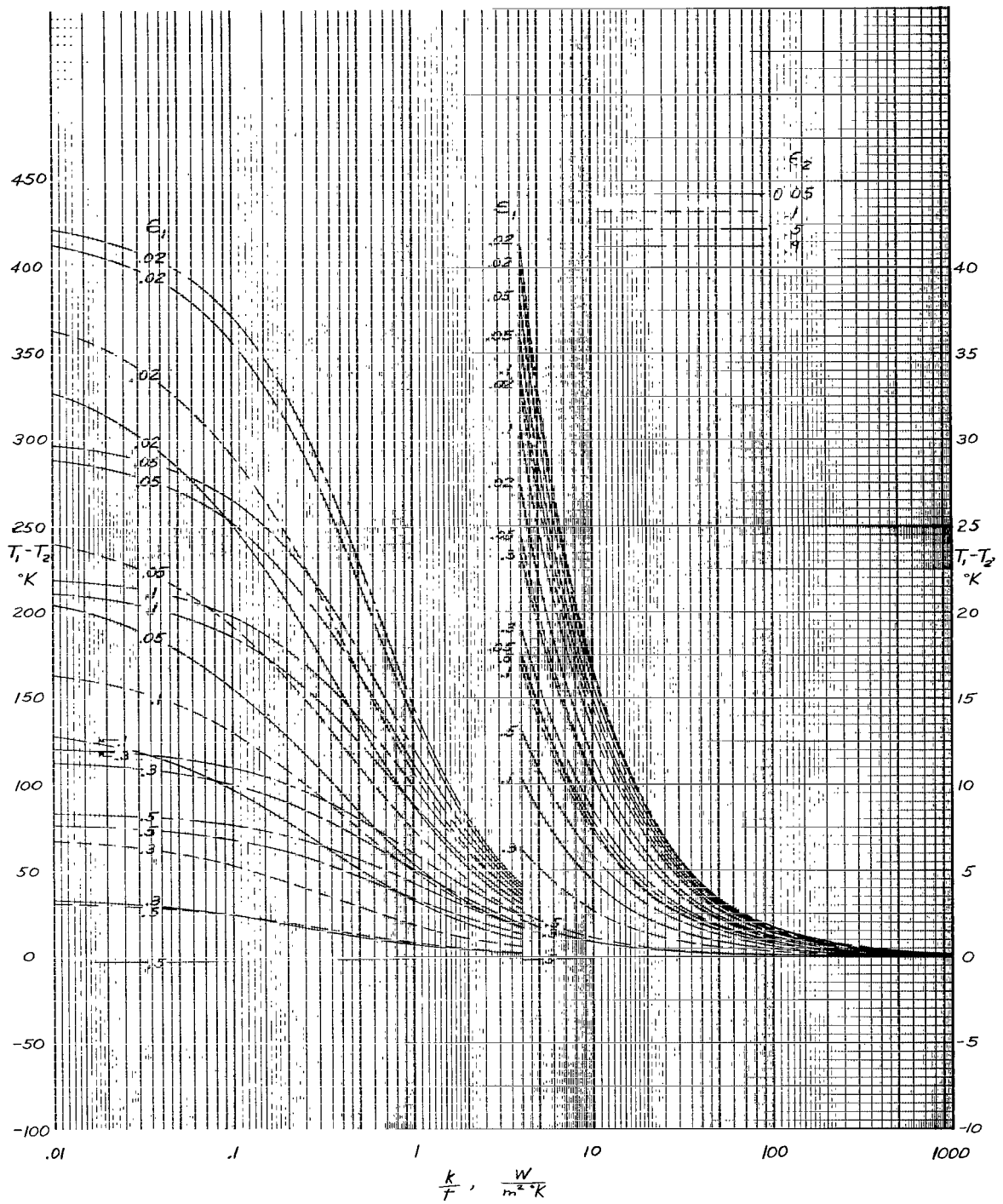


Figure 7.- Front-surface temperature of a paraboloidal mirror. $h = 500 \text{ km}$; $\alpha_2 = \epsilon_2 = 0.9$; $\theta_R = 60^\circ$.



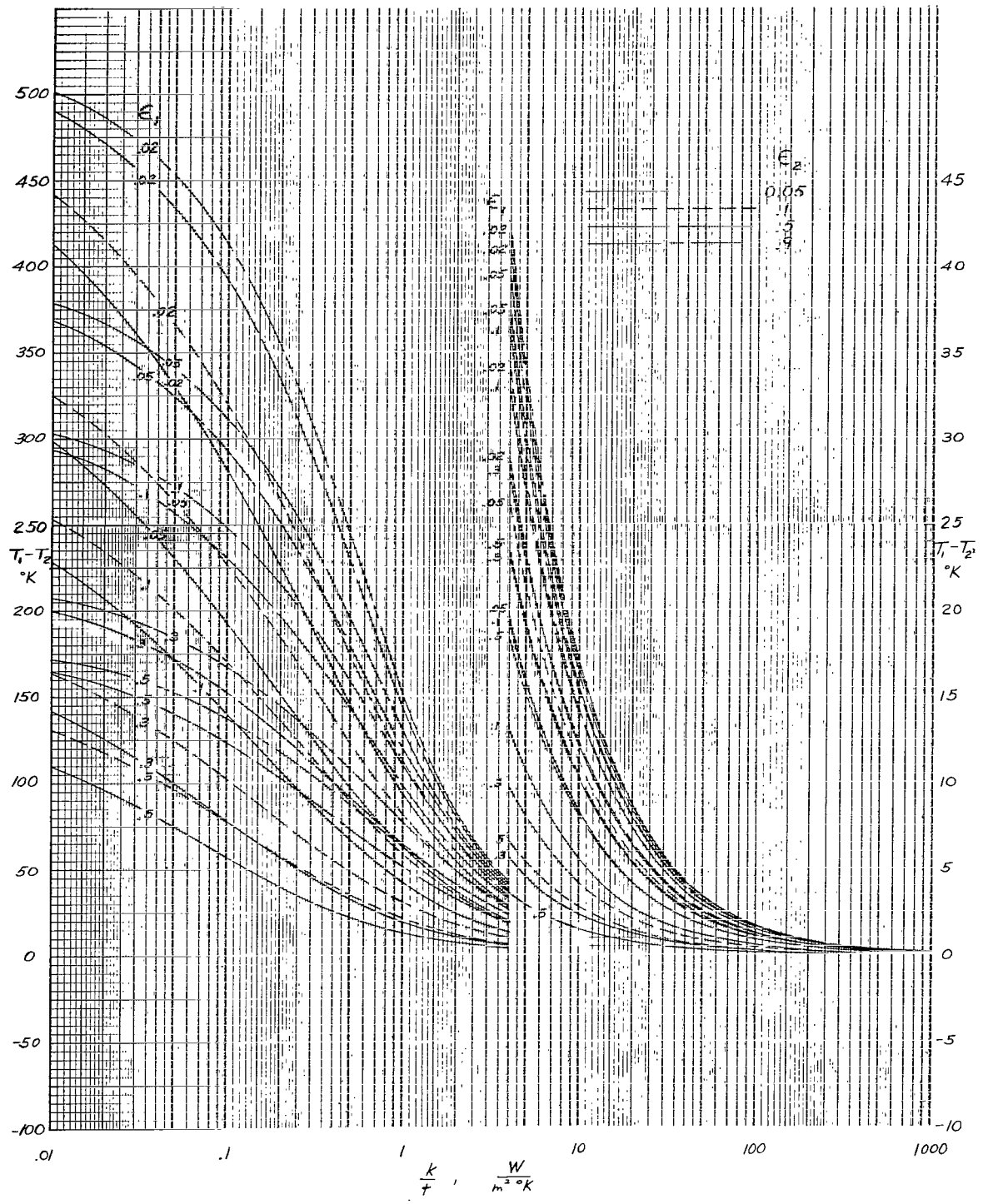
(a) $h = 500$ km.

Figure 8.- Temperature difference between front and rear surfaces of paraboloidal mirror for near-earth case. $\alpha_1 = 0.125$; $\alpha_2 = 0.1$; $\theta_R = 60^\circ$.



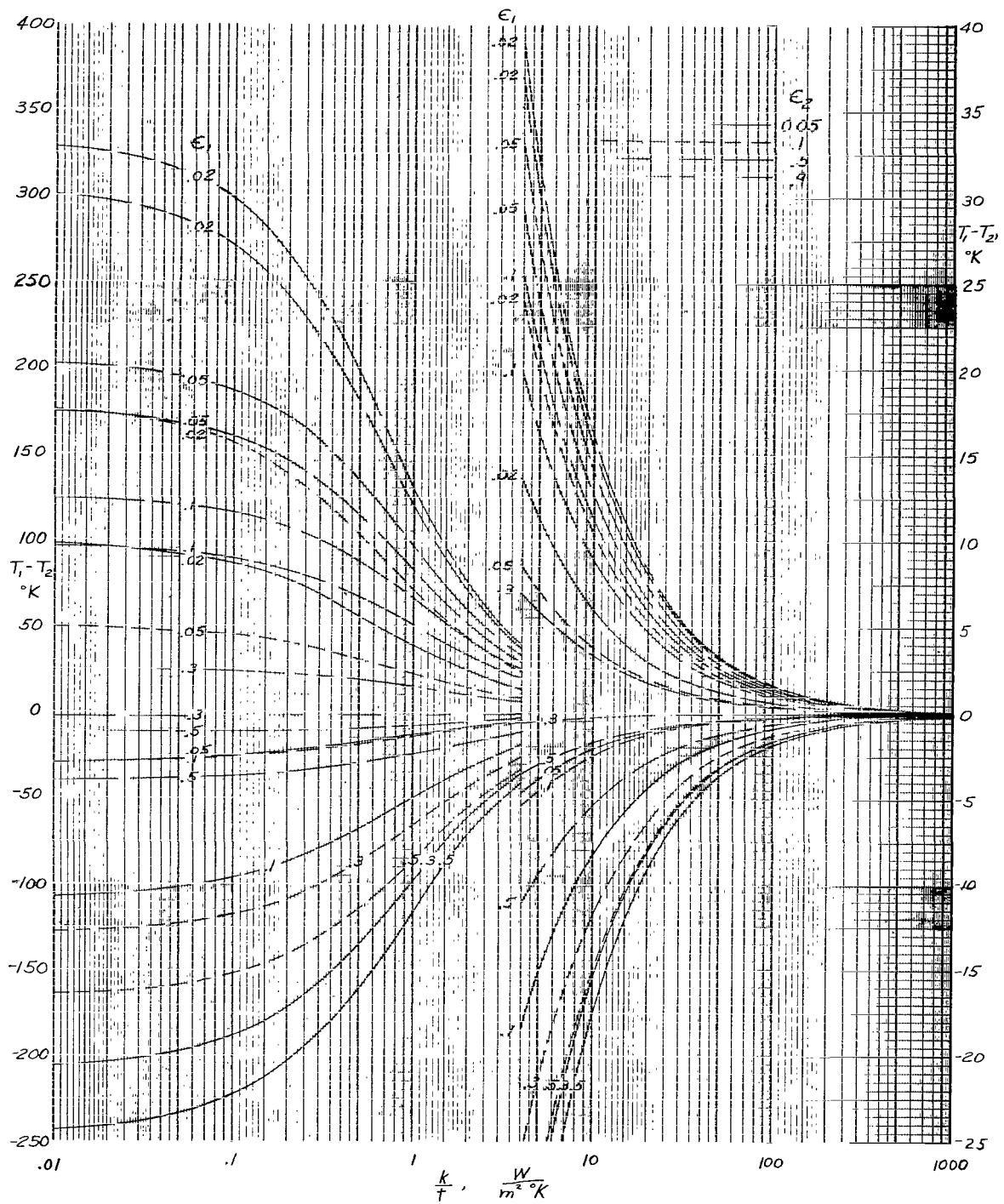
(b) $h = 5000$ km.

Figure 8.- Continued.



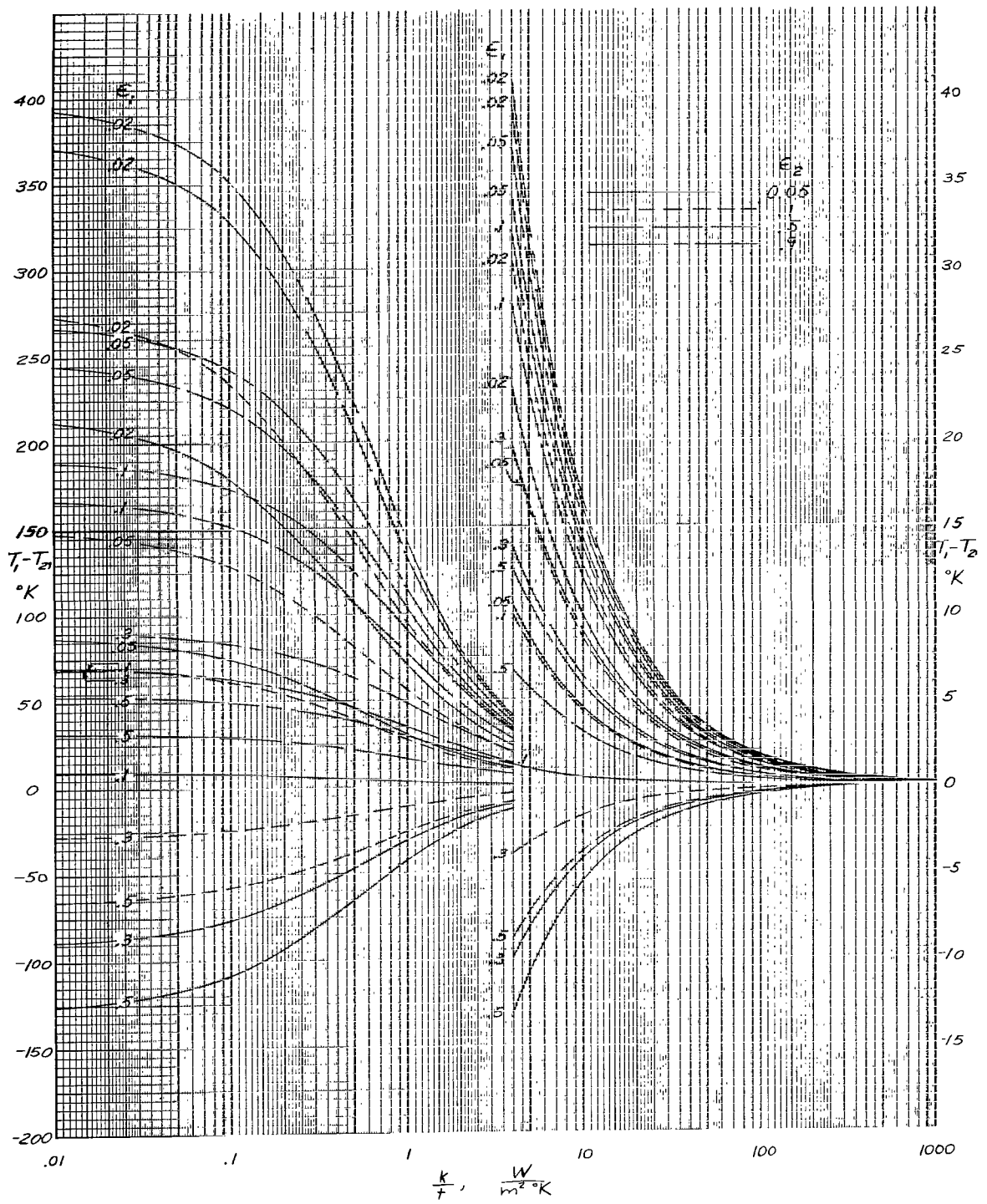
(c) $h = 35\ 000\ \text{km}$.

Figure 8.- Concluded.



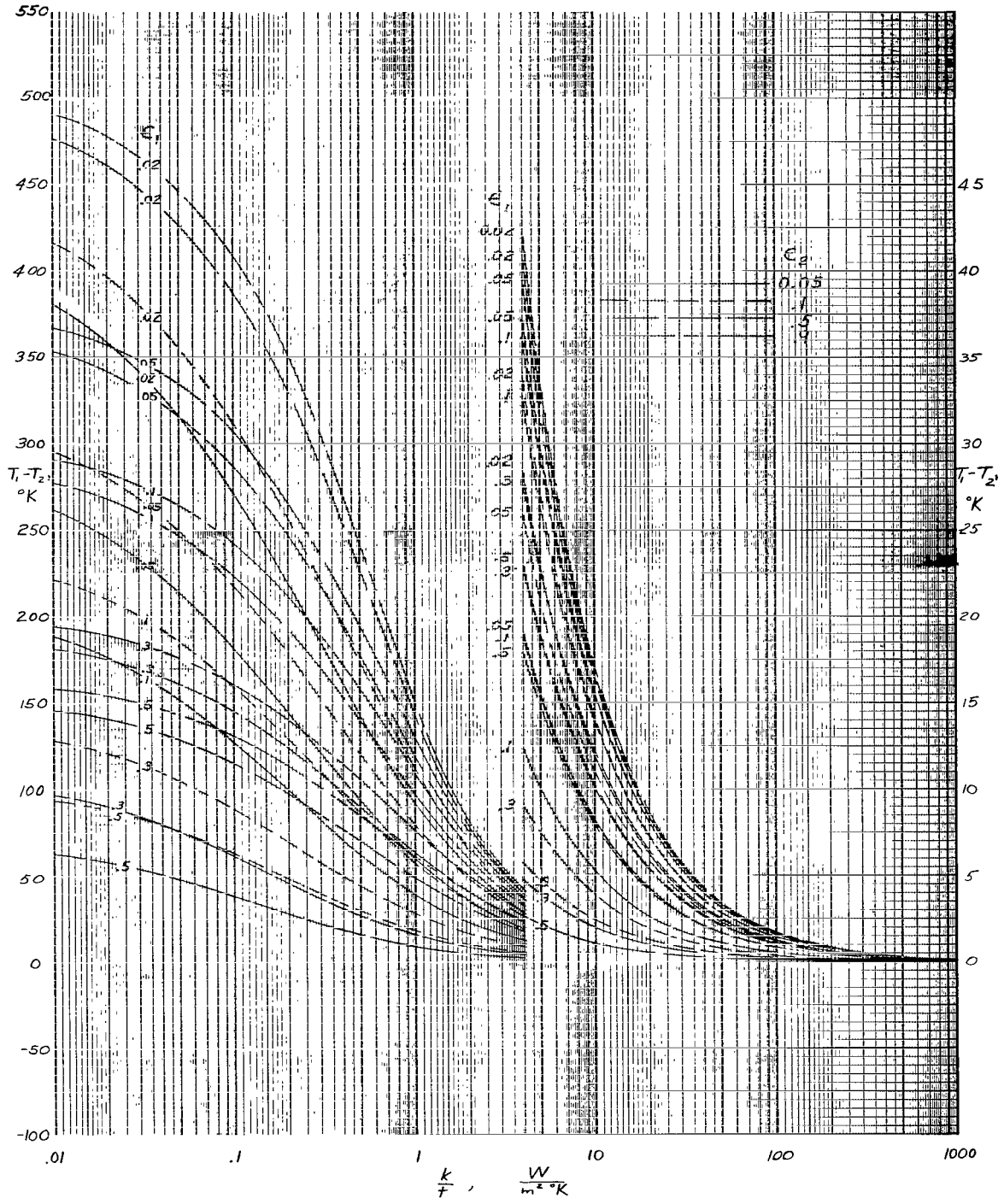
(a) $h = 500$ km.

Figure 9.- Temperature difference between front and rear surfaces of paraboloidal mirror for near-earth case. $\alpha_1 = 0.125$; $\alpha_2 = 0.5$; $\theta_R = 60^\circ$.



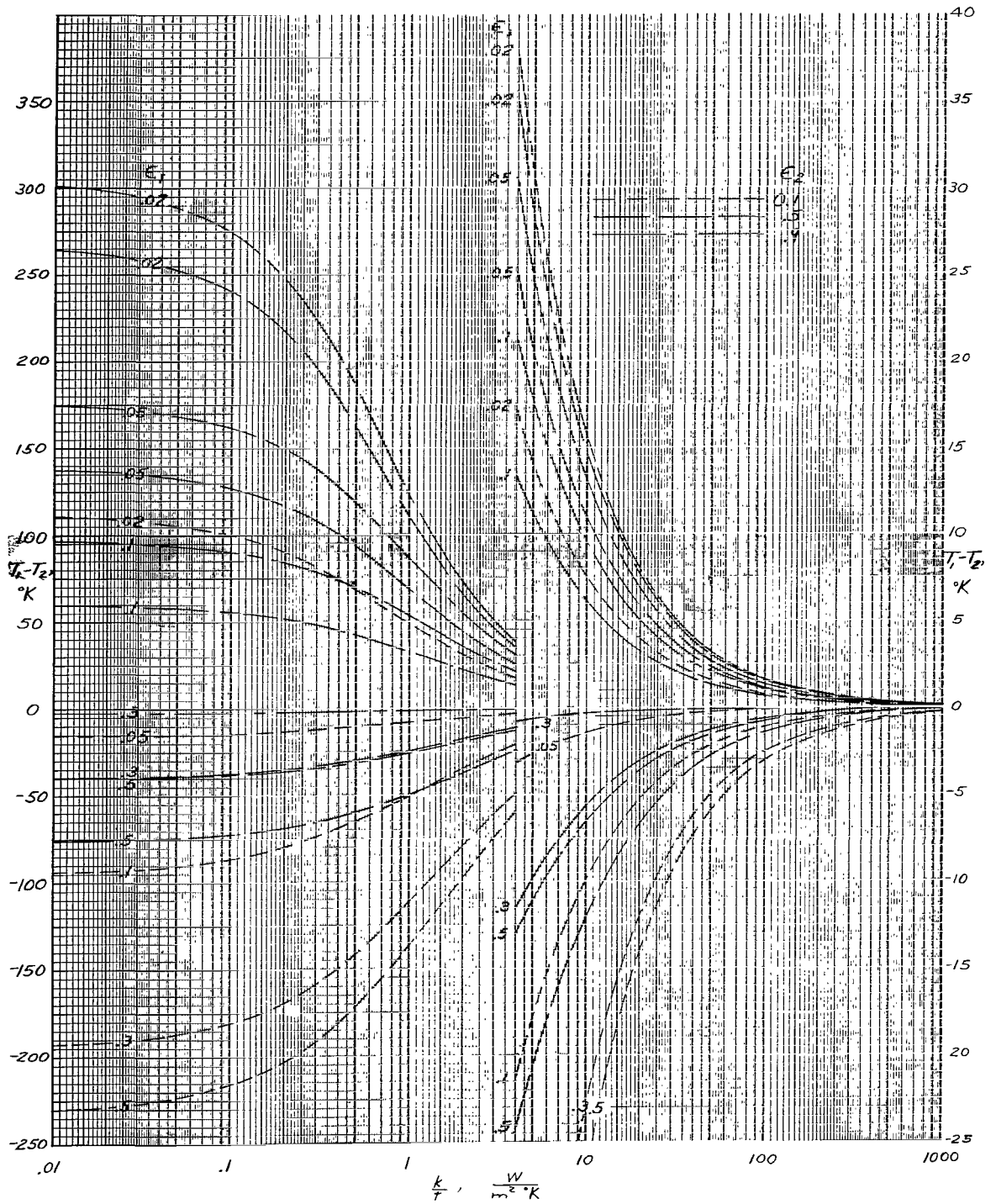
(b) $h = 5000$ km.

Figure 9.- Continued.



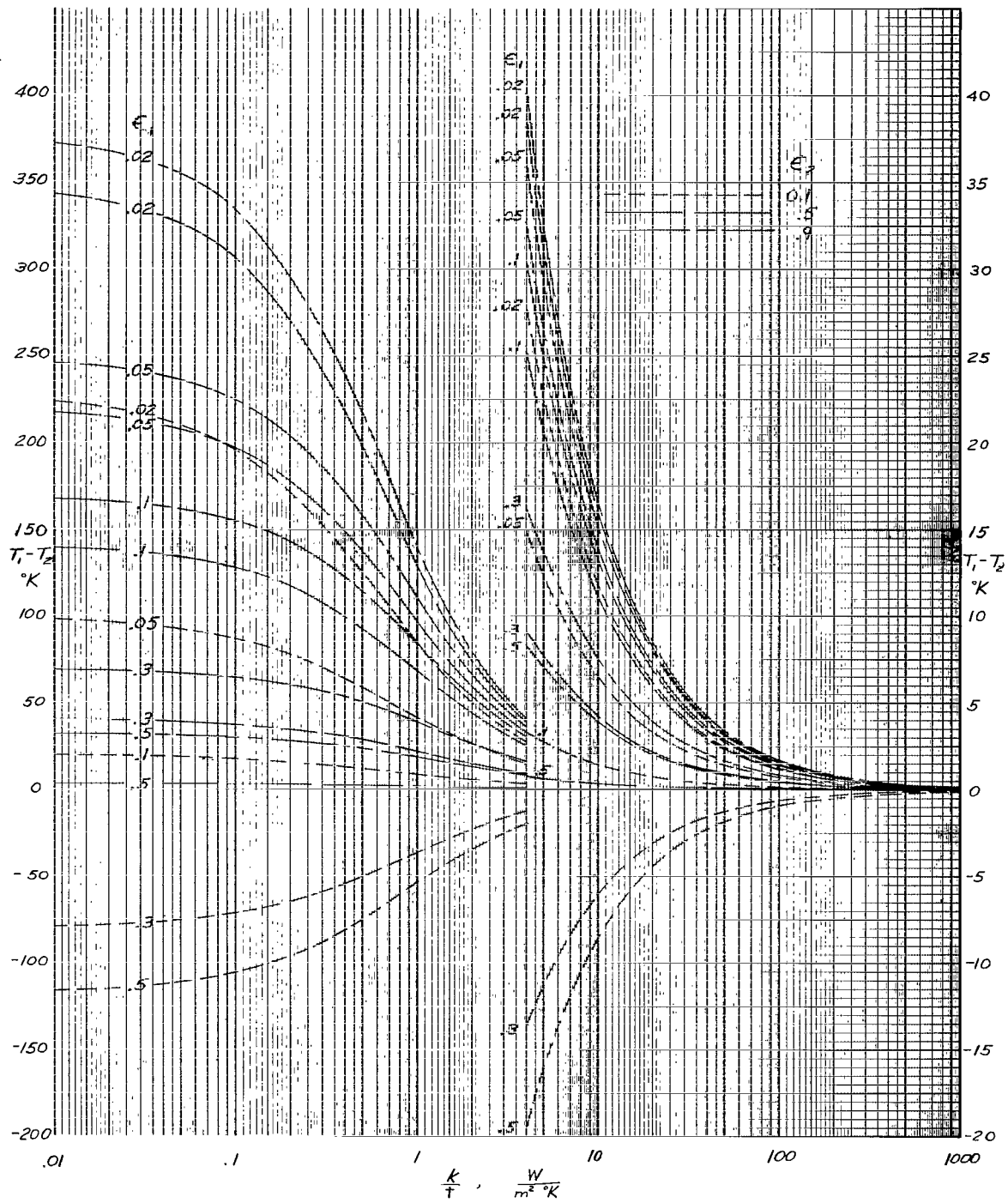
(c) $h = 35\,000 \text{ km}$.

Figure 9.- Concluded.



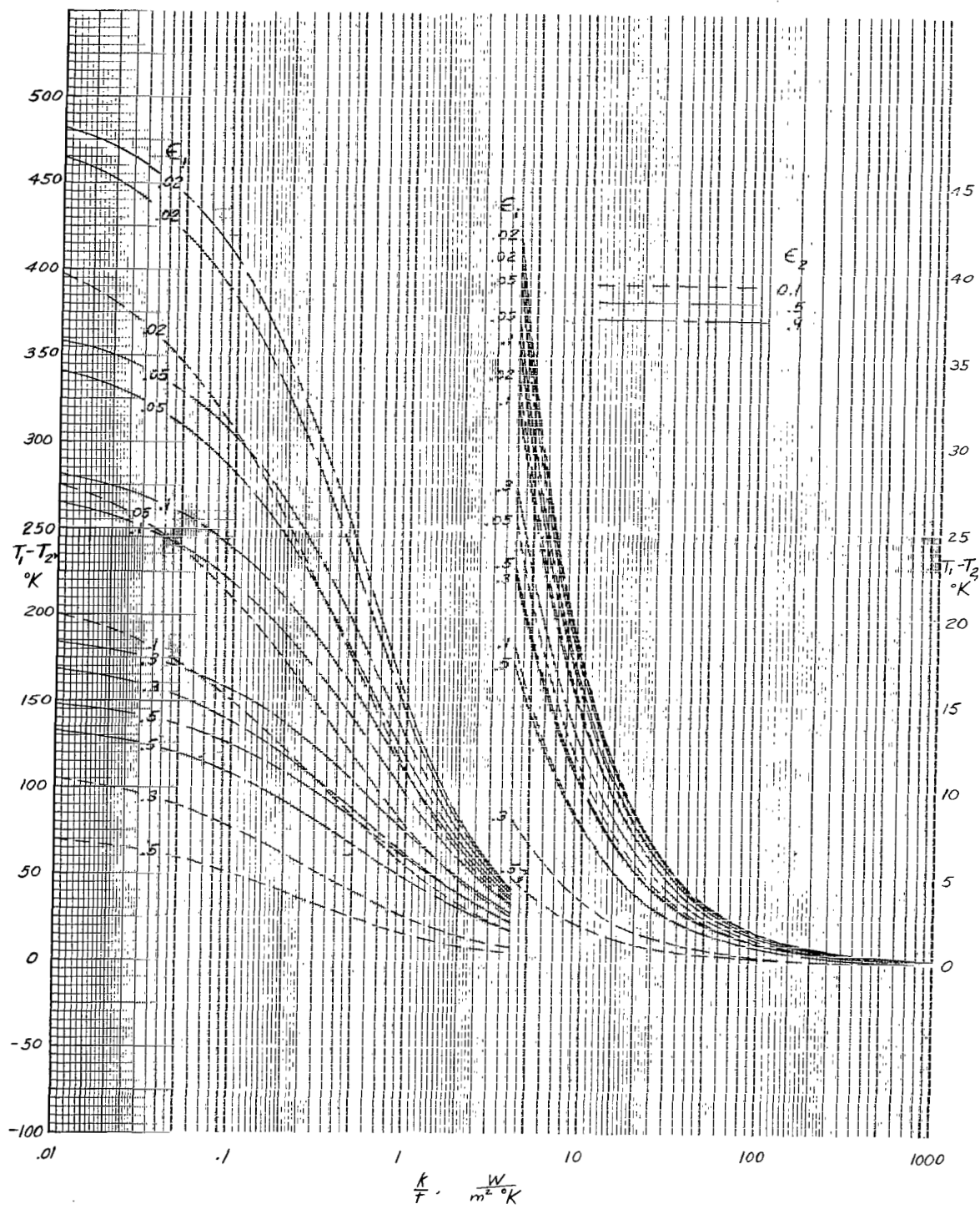
(a) $h = 500$ km.

Figure 10.- Temperature difference between front and rear surfaces of paraboloidal mirror for near-earth case. $\alpha_1 = 0.125$; $\alpha_2 = 0.9$; $\theta_R = 60^\circ$.



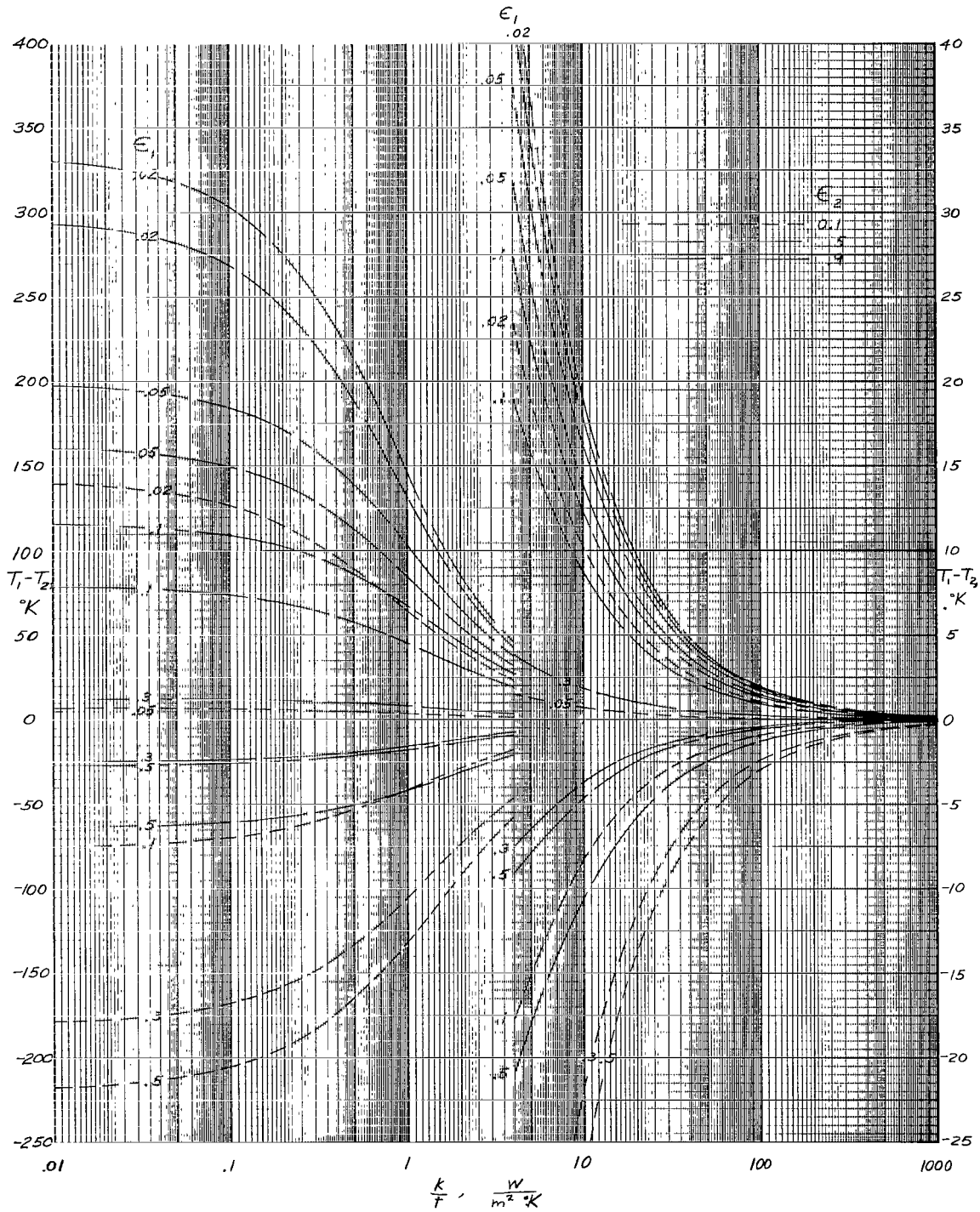
(b) $h = 5000$ km.

Figure 10.- Continued.



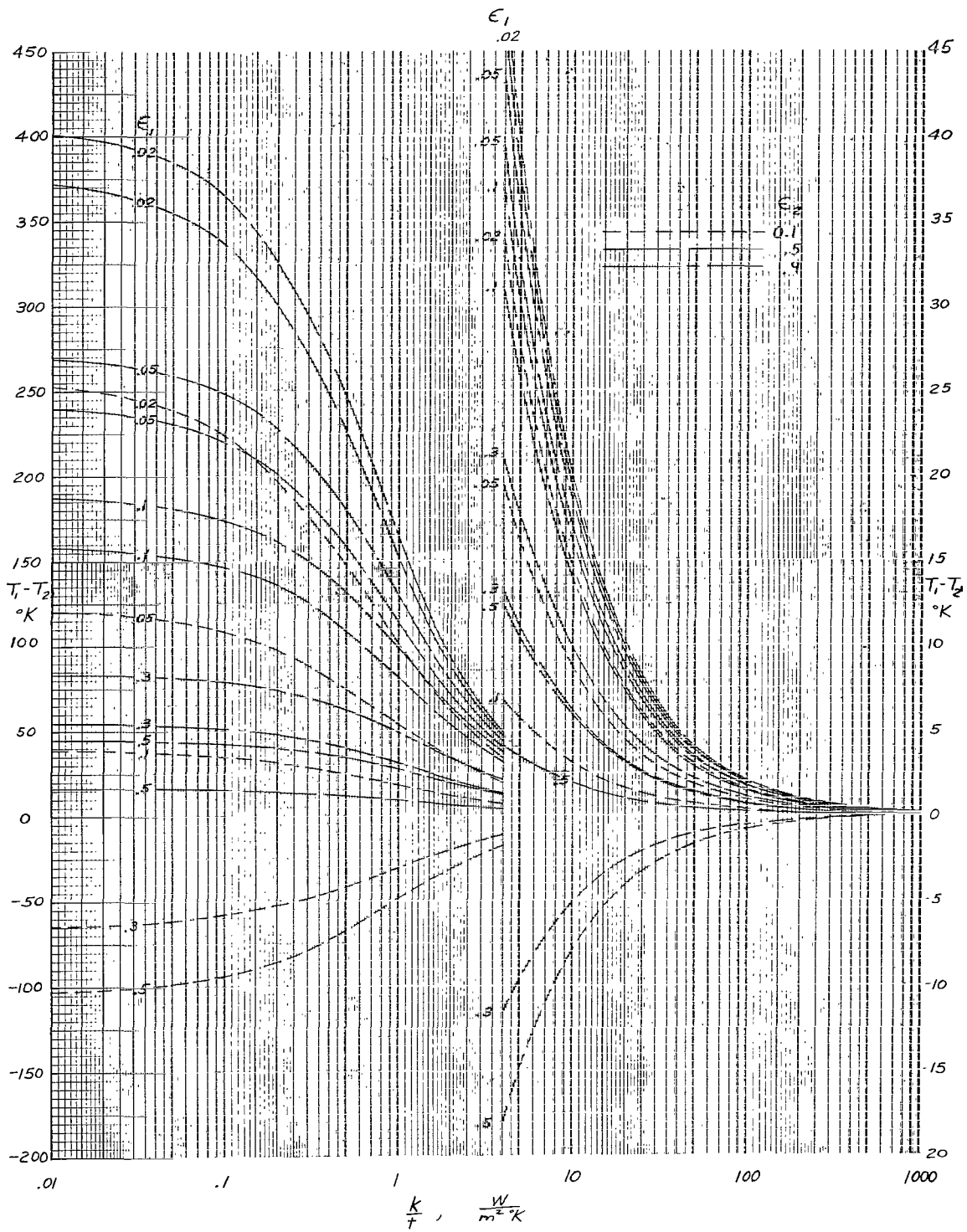
(c) $h = 35\ 000\ \text{km}$.

Figure 10.- Concluded.



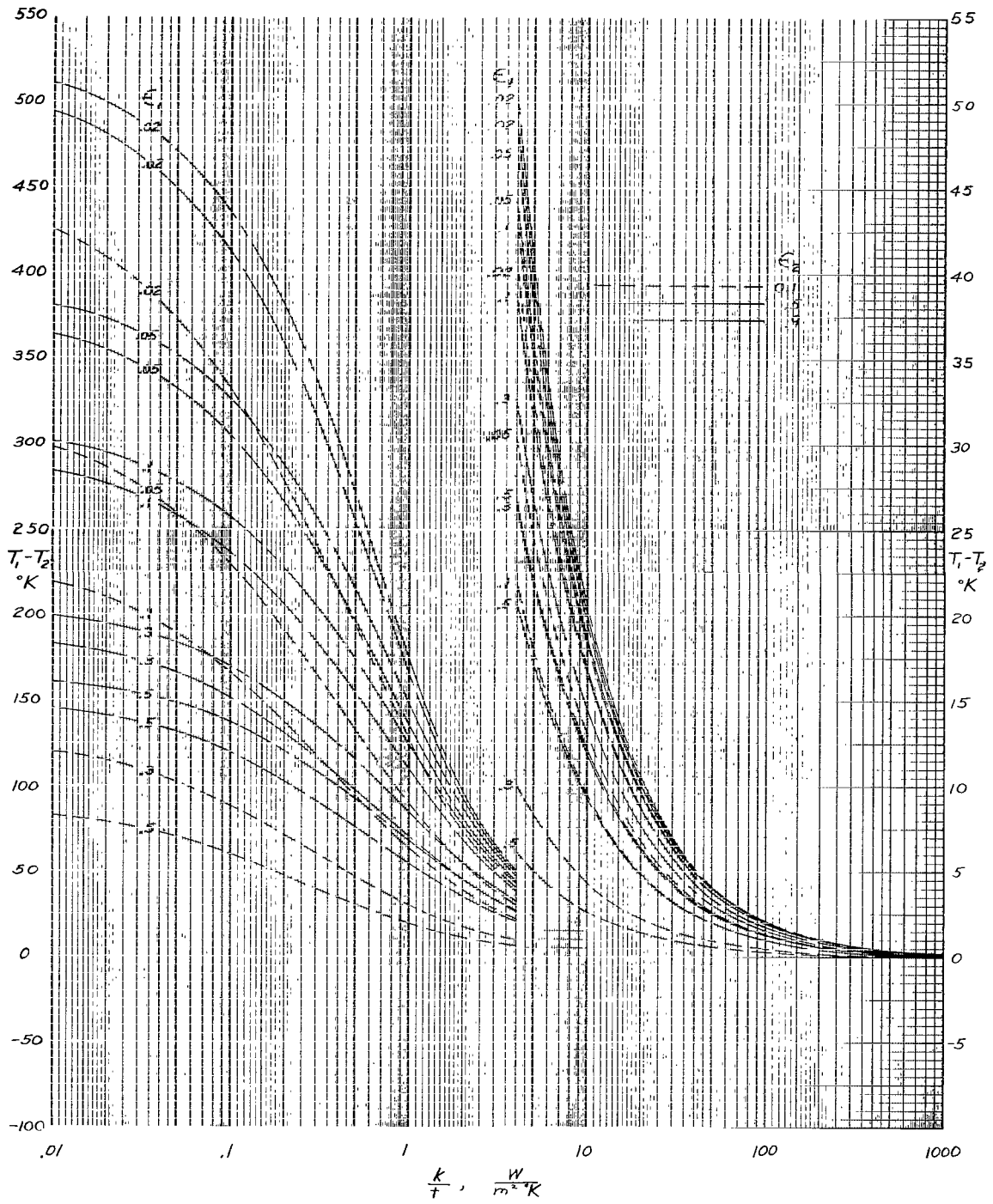
(a) $h = 500$ km.

Figure 11.- Temperature difference between front and rear surfaces of paraboloidal mirror for near-earth case. $\alpha_1 = 0.15$; $\alpha_2 = 0.9$; $\theta_R = 60^\circ$.



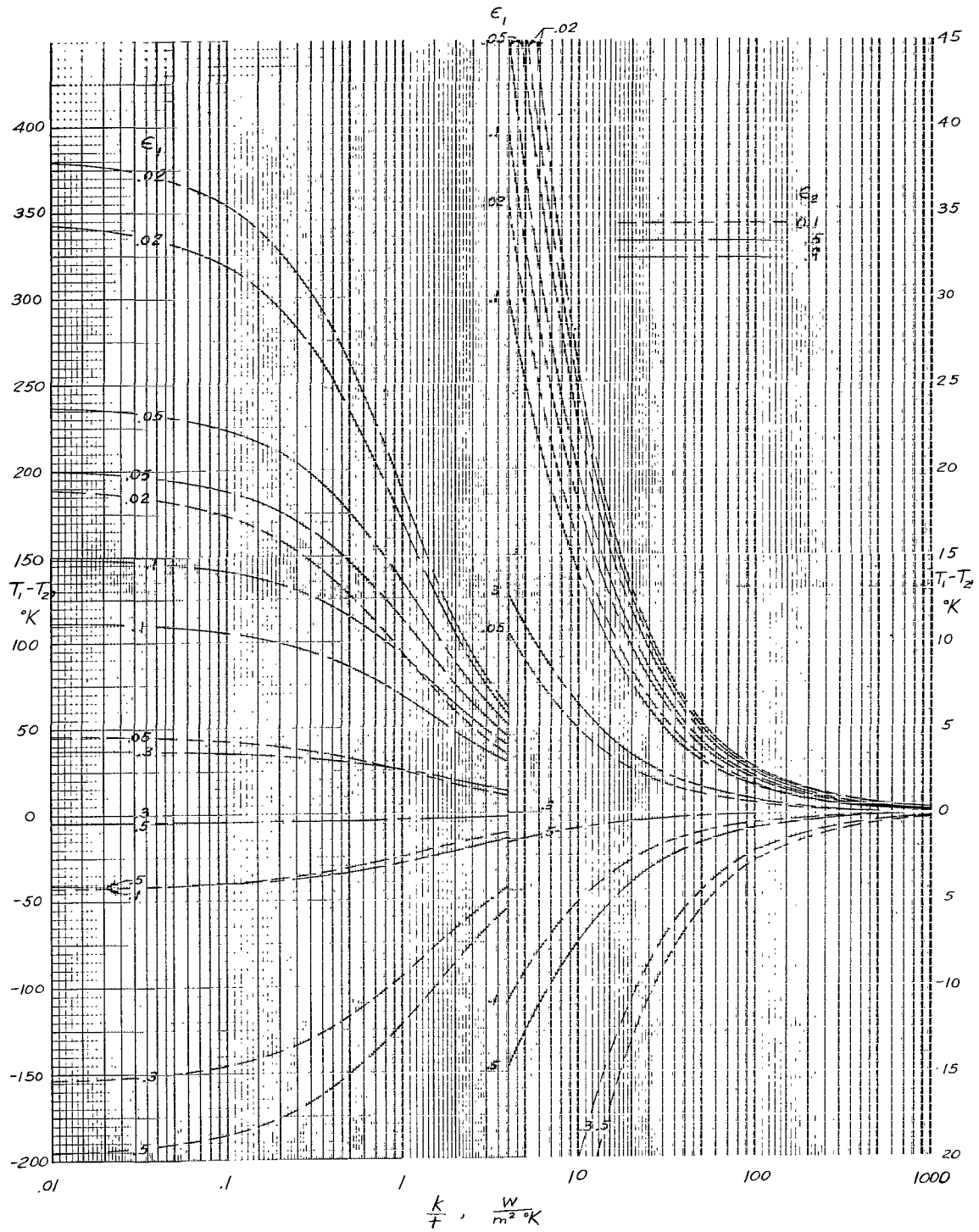
(b) $h = 5000 \text{ km}$.

Figure 11.- Continued.



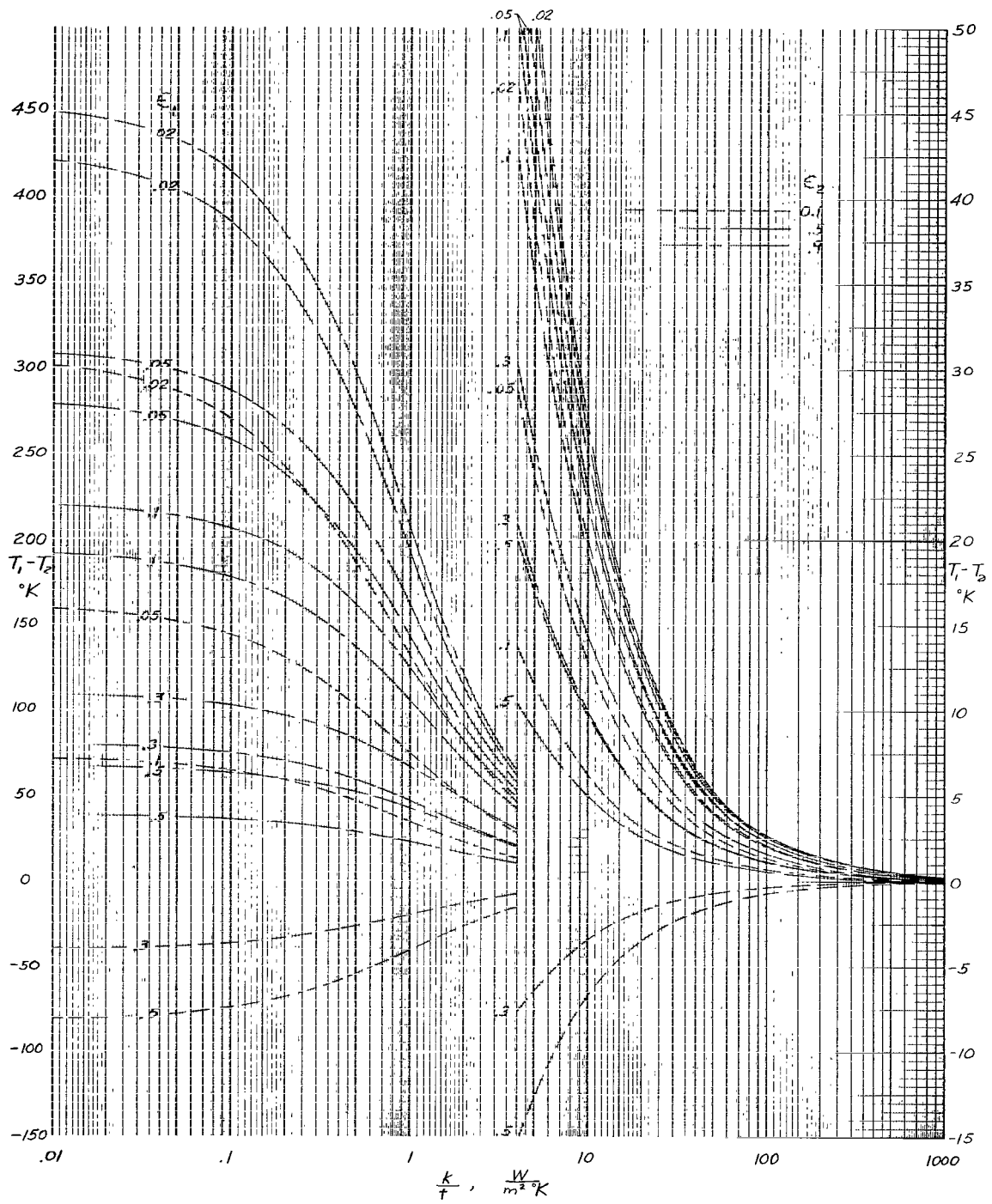
(c) $h = 35\,000$ km.

Figure 11.- Concluded.



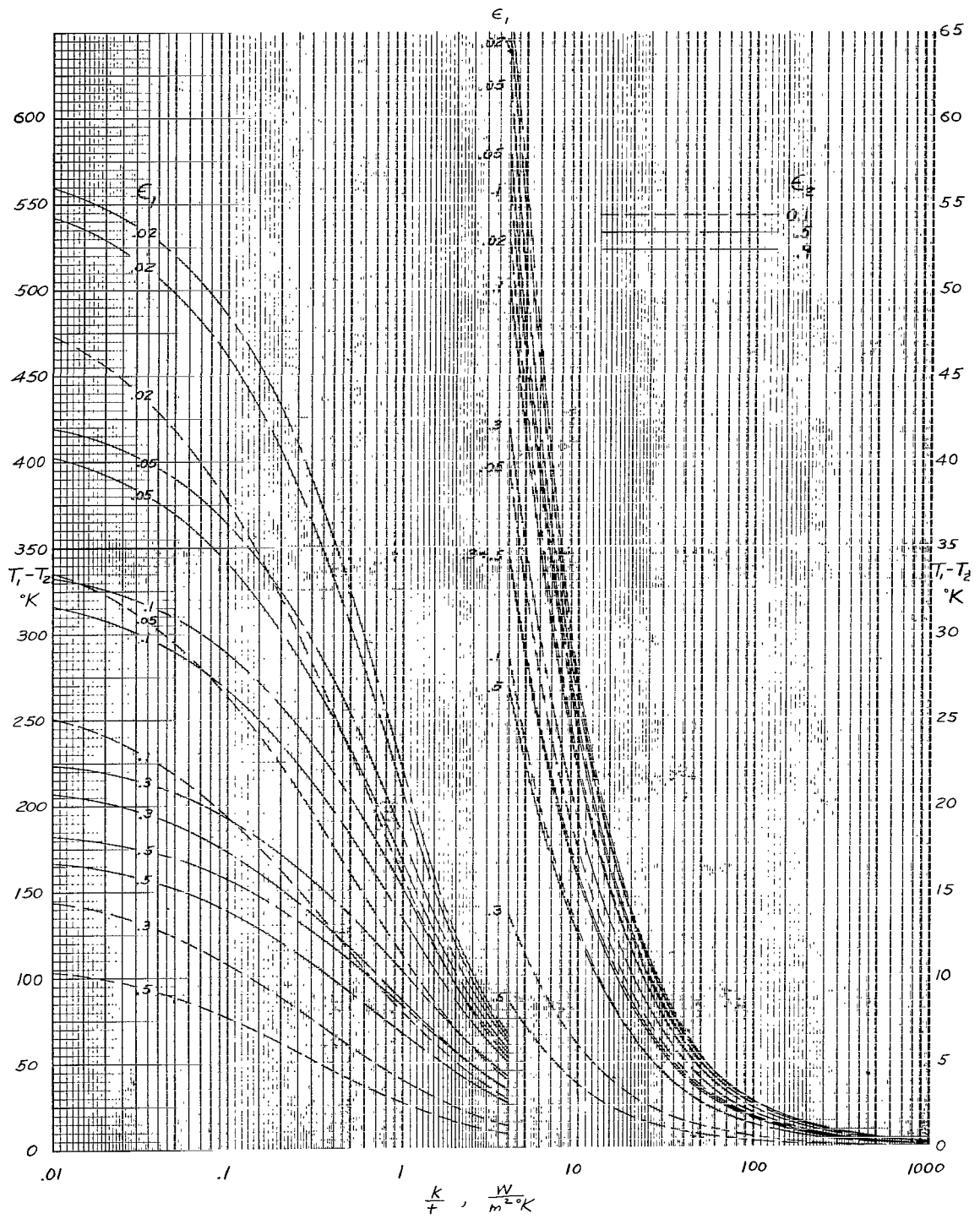
(a) $h = 500$ km.

Figure 12.- Temperature difference between front and rear surfaces of paraboloidal mirror for near-earth case. $\alpha_1 = 0.2$; $\alpha_2 = 0.9$; $\theta_R = 60^\circ$.



(b) $h = 5000$ km.

Figure 12.- Continued.



(c) $h = 35\ 000\ km.$

Figure 12.- Concluded.

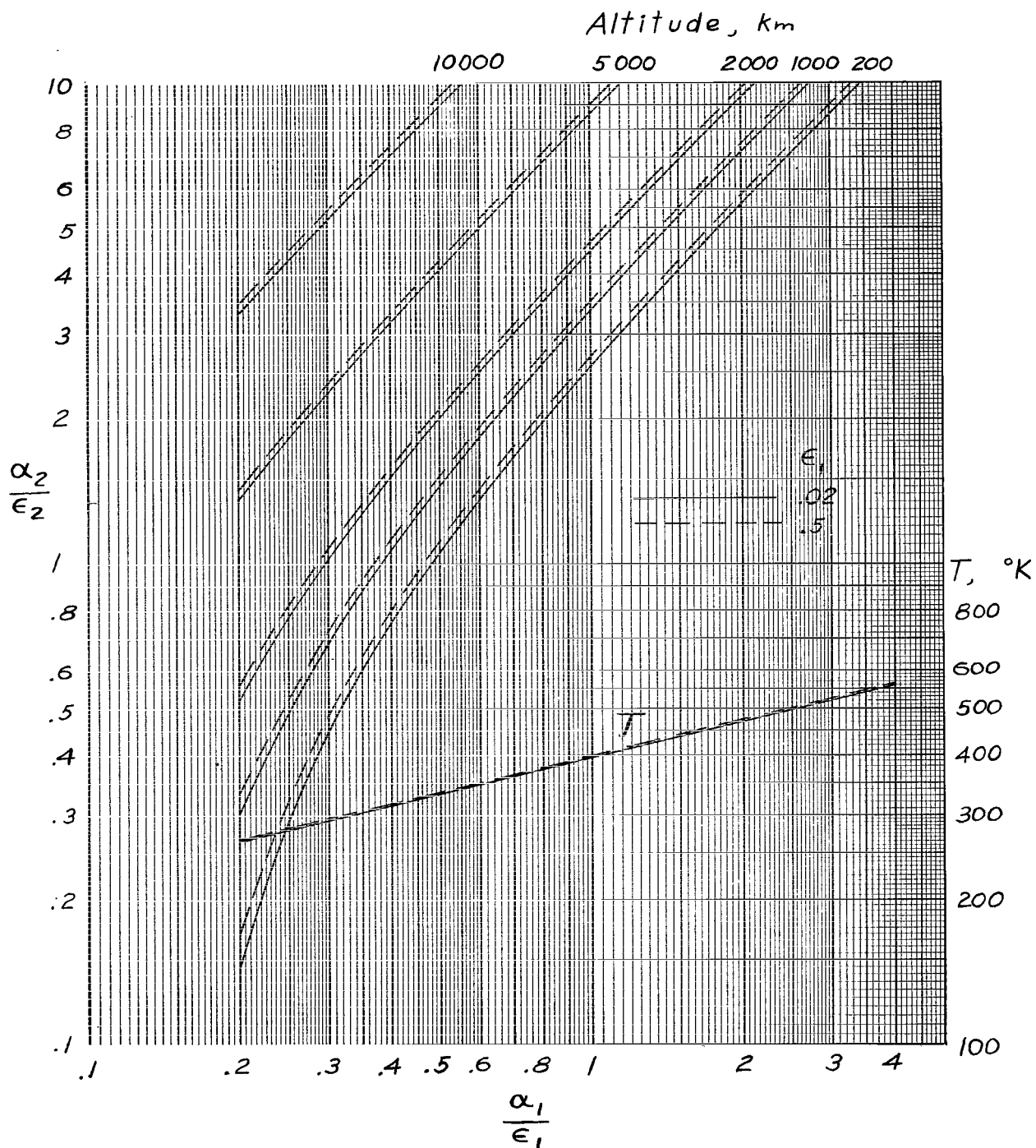
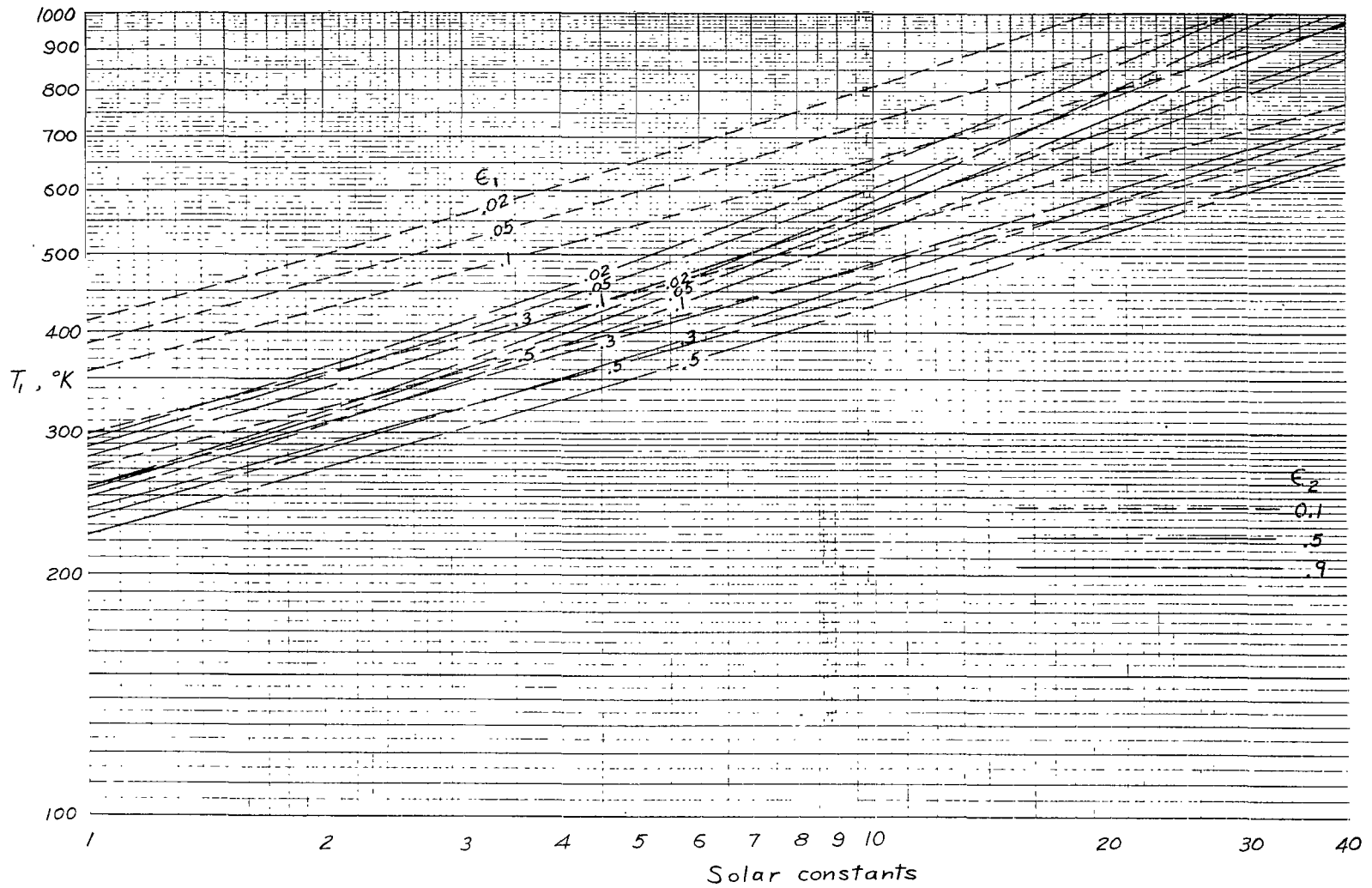
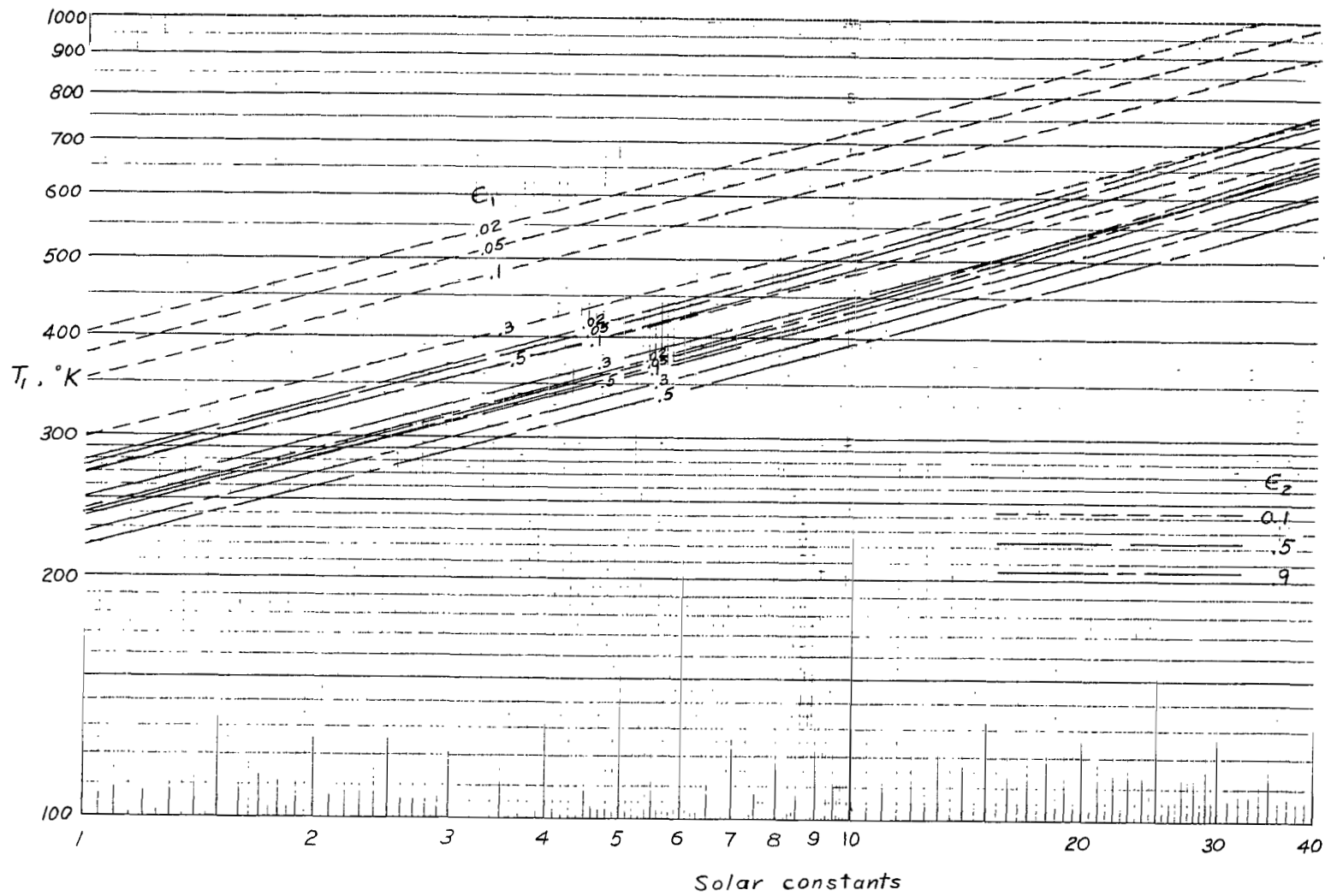


Figure 13.- Ratios of absorptance to emittance required for zero temperature gradient through paraboloidal mirror. $\theta_R = 60^\circ$.



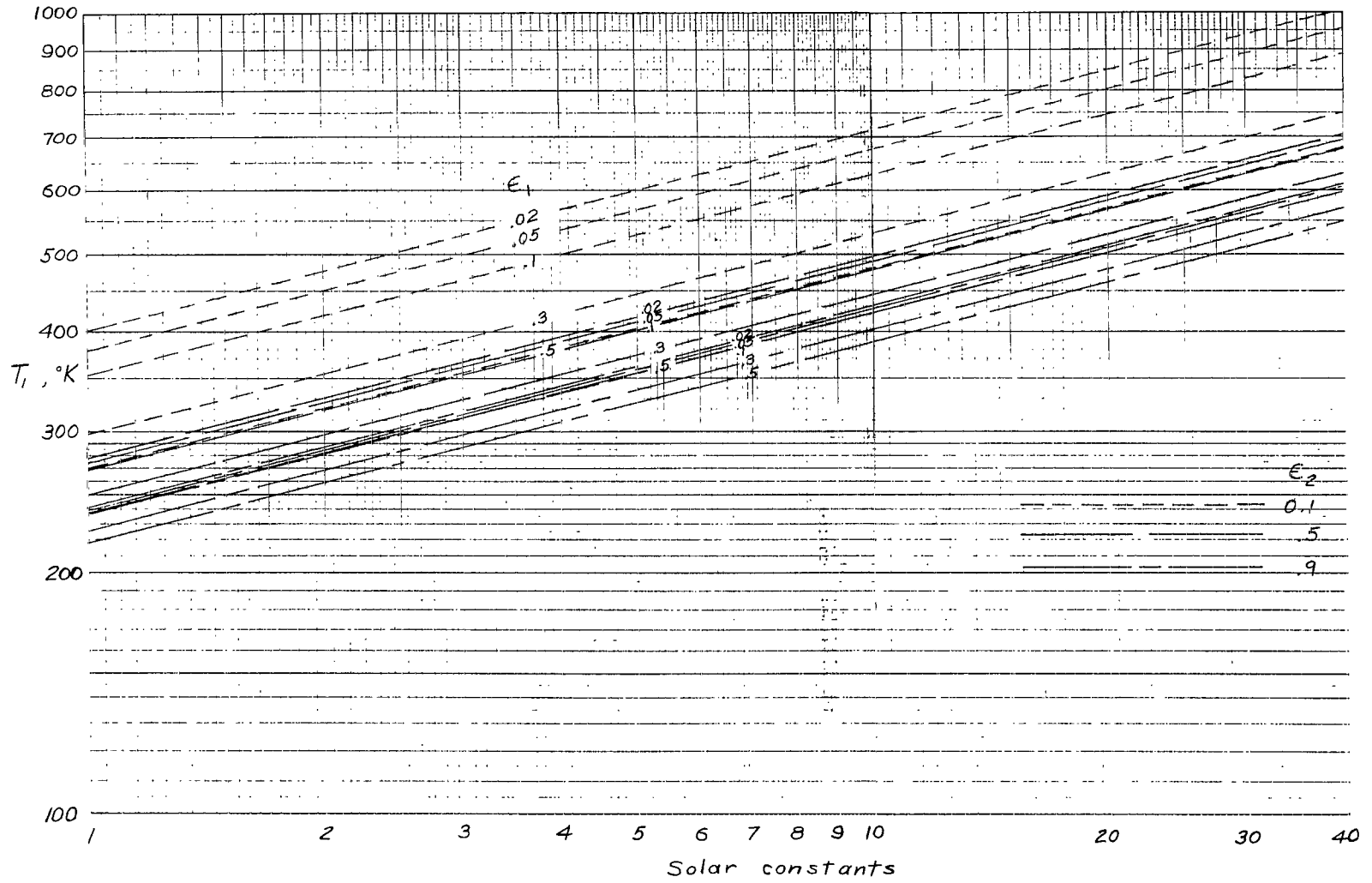
(a) $\frac{k}{t} = 10$.

Figure 14.- Front-surface temperature of paraboloidal mirror for solar-probe case. $\alpha_1 = 0.125$; $\theta_R = 60^\circ$.



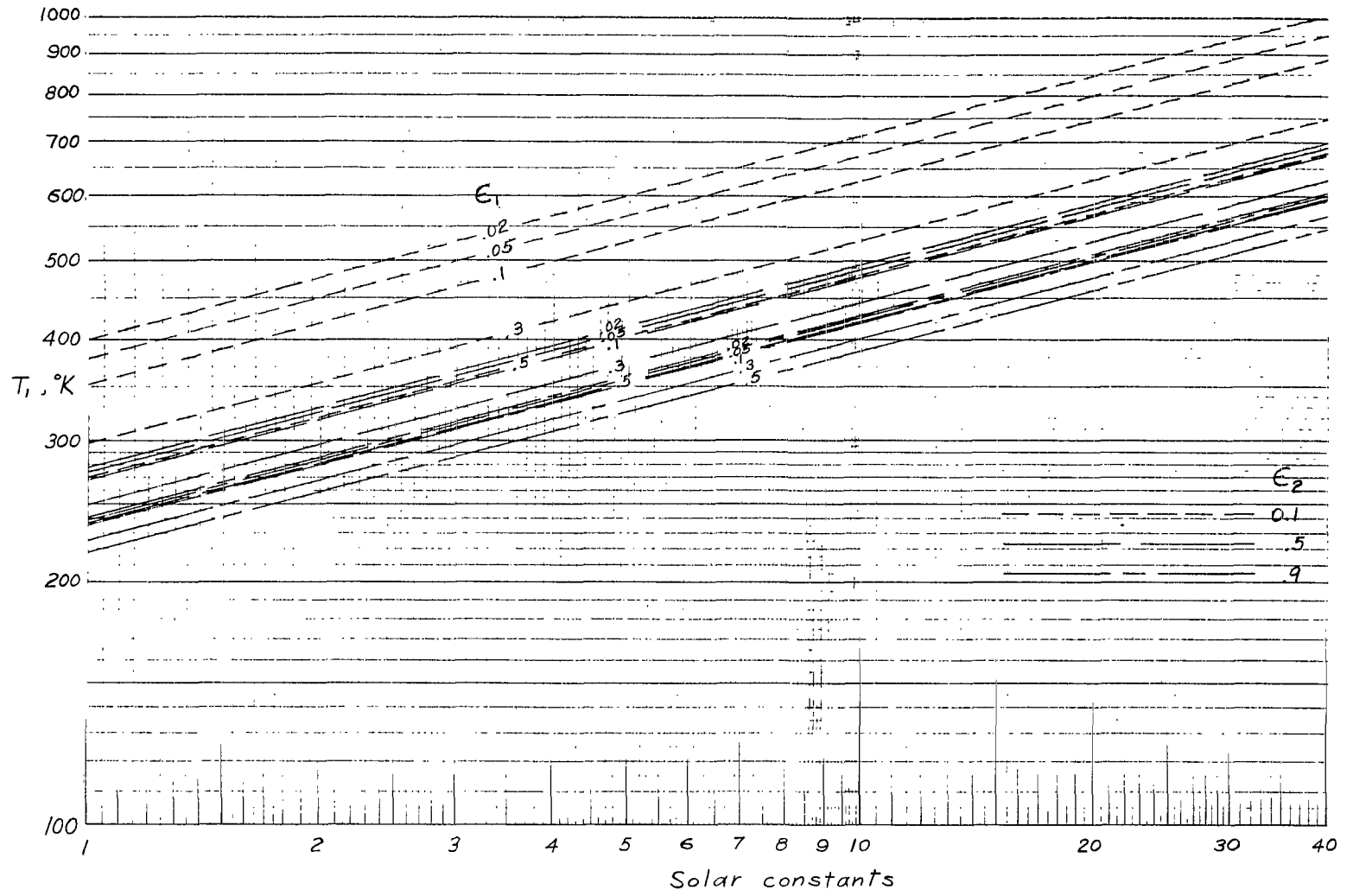
(b) $\frac{k}{t} = 100.$

Figure 14.- Continued.



(c) $\frac{k}{t} = 1000$.

Figure 14.- Continued.



(d) $\frac{k}{t} = 10\ 000.$

Figure 14.- Concluded.

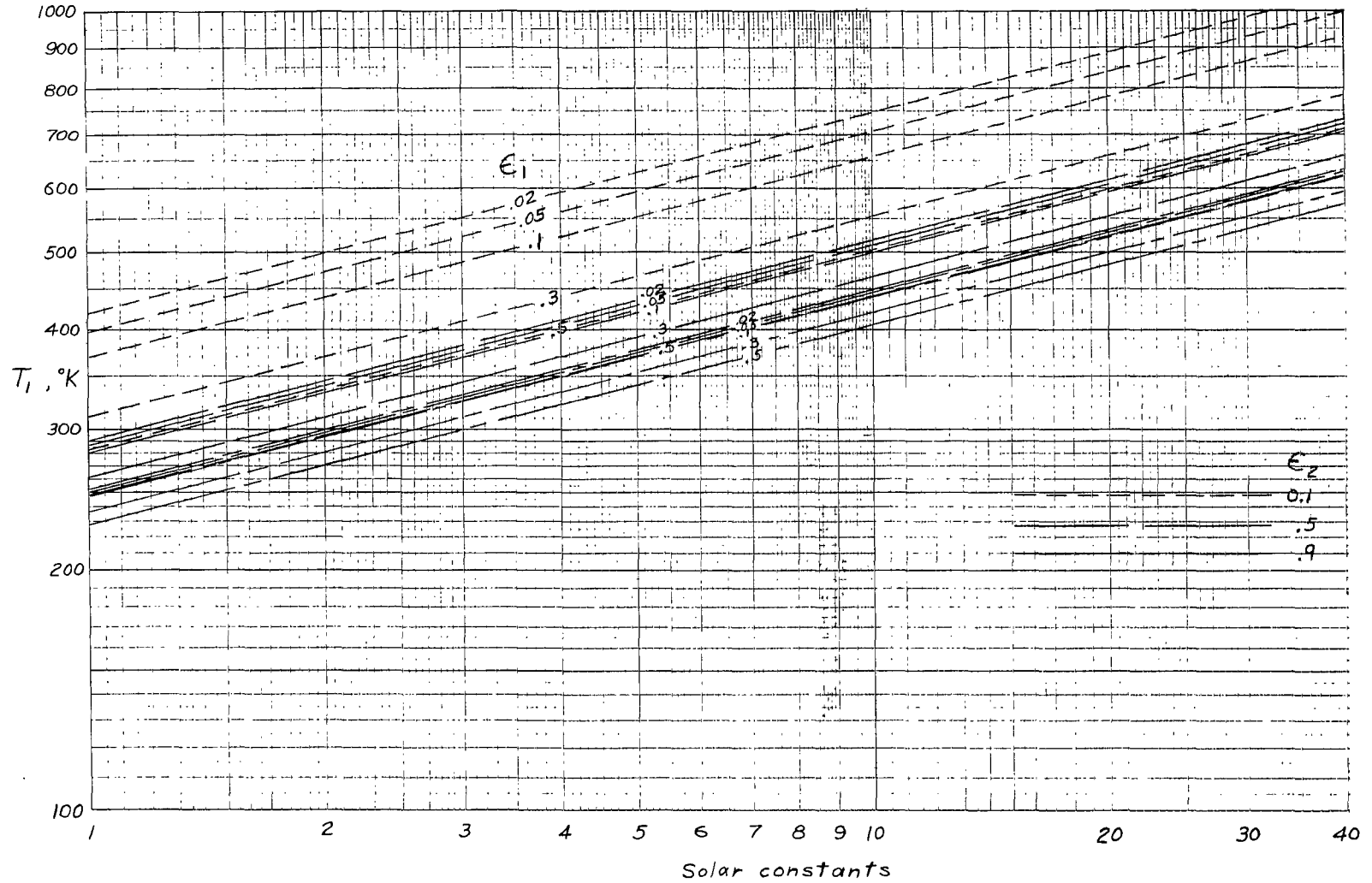


Figure 15.- Front-surface temperature of paraboloidal mirror for solar-probe case. $\alpha_1 = 0.15$; $\frac{k}{t} = 10\ 000$; $\theta_R = 60^\circ$.

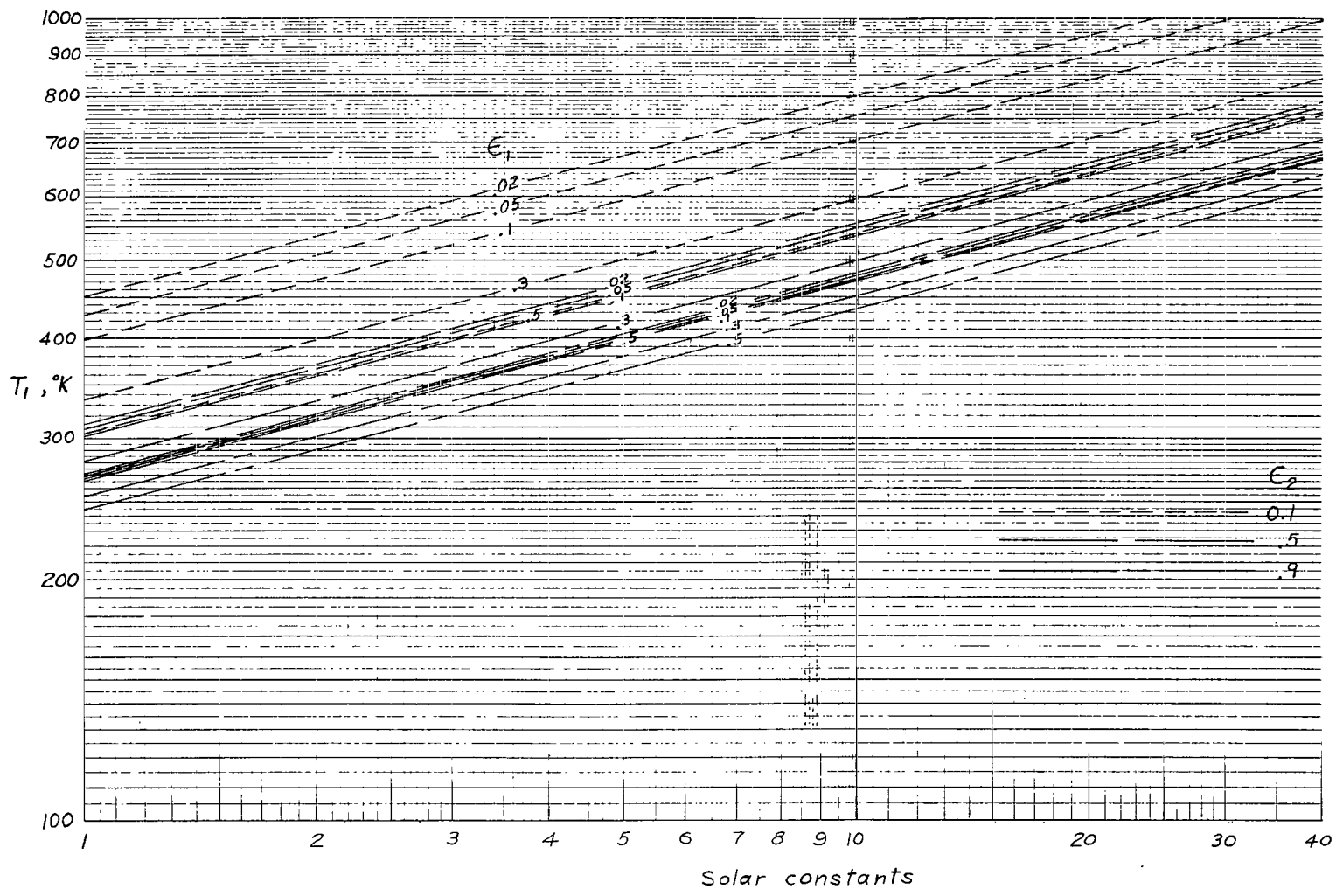
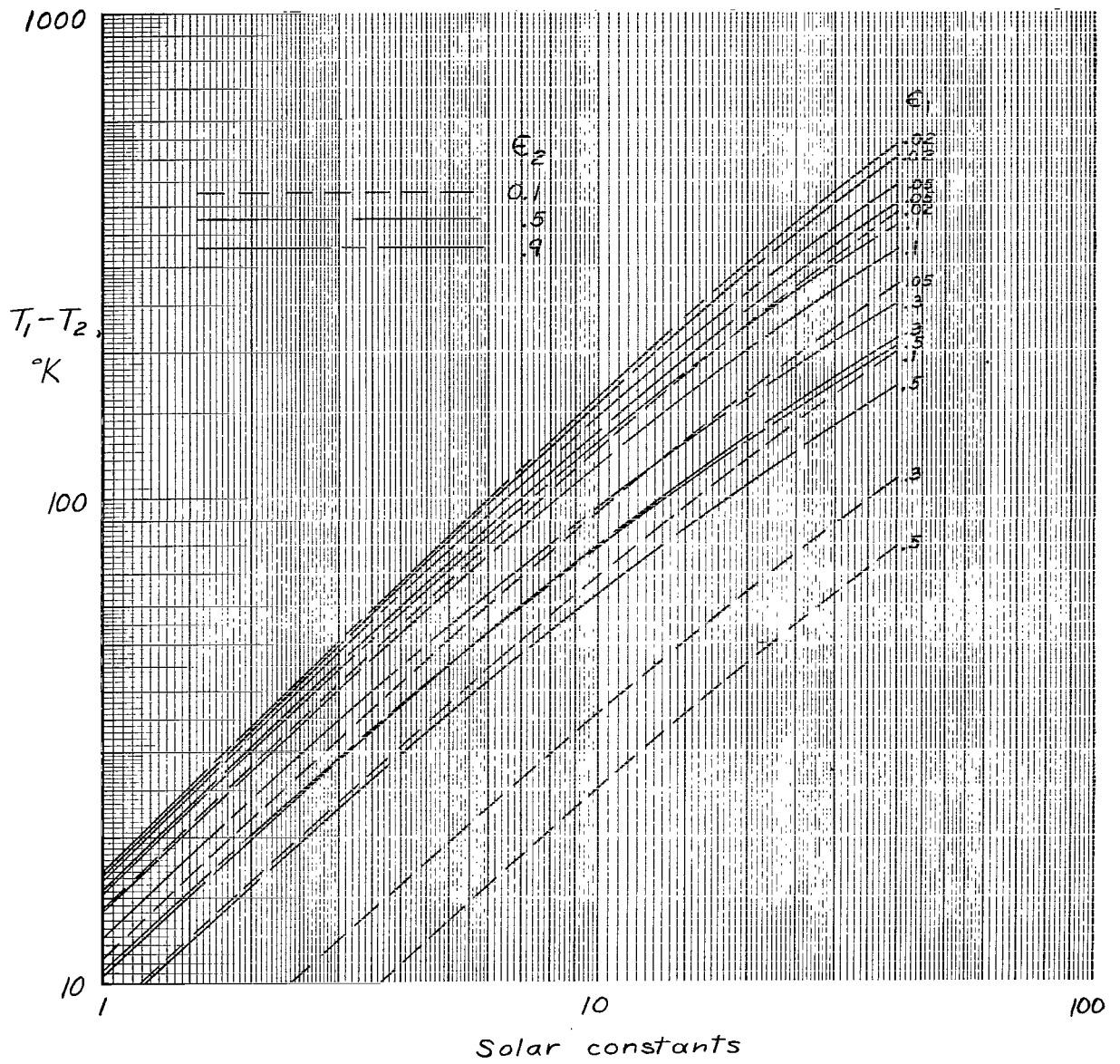
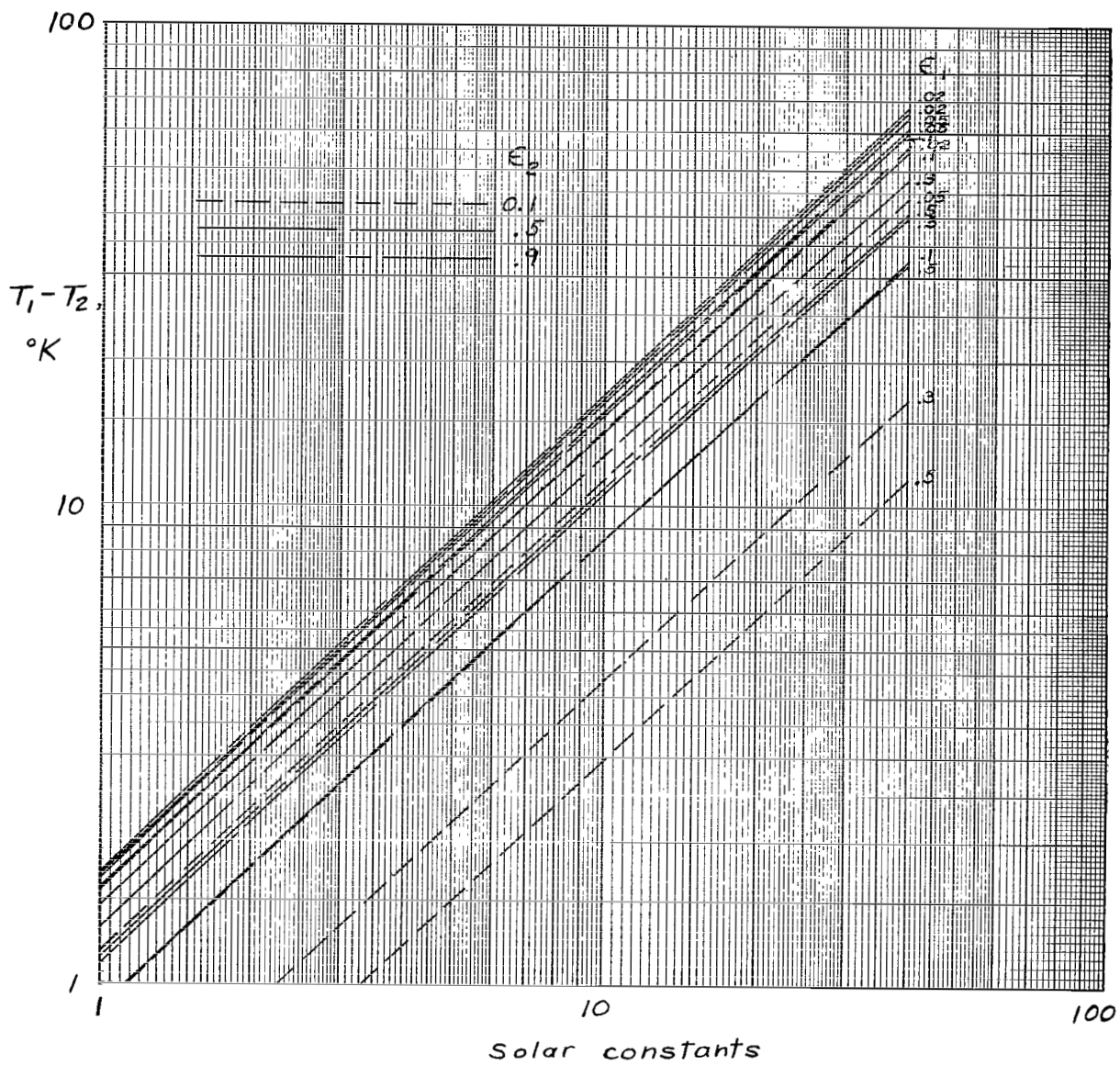


Figure 16.- Front-surface temperature of paraboloidal mirror for solar-probe case. $\alpha_1 = 0.2$; $\frac{k}{t} = 10\ 000$; $\theta_R = 60^\circ$.

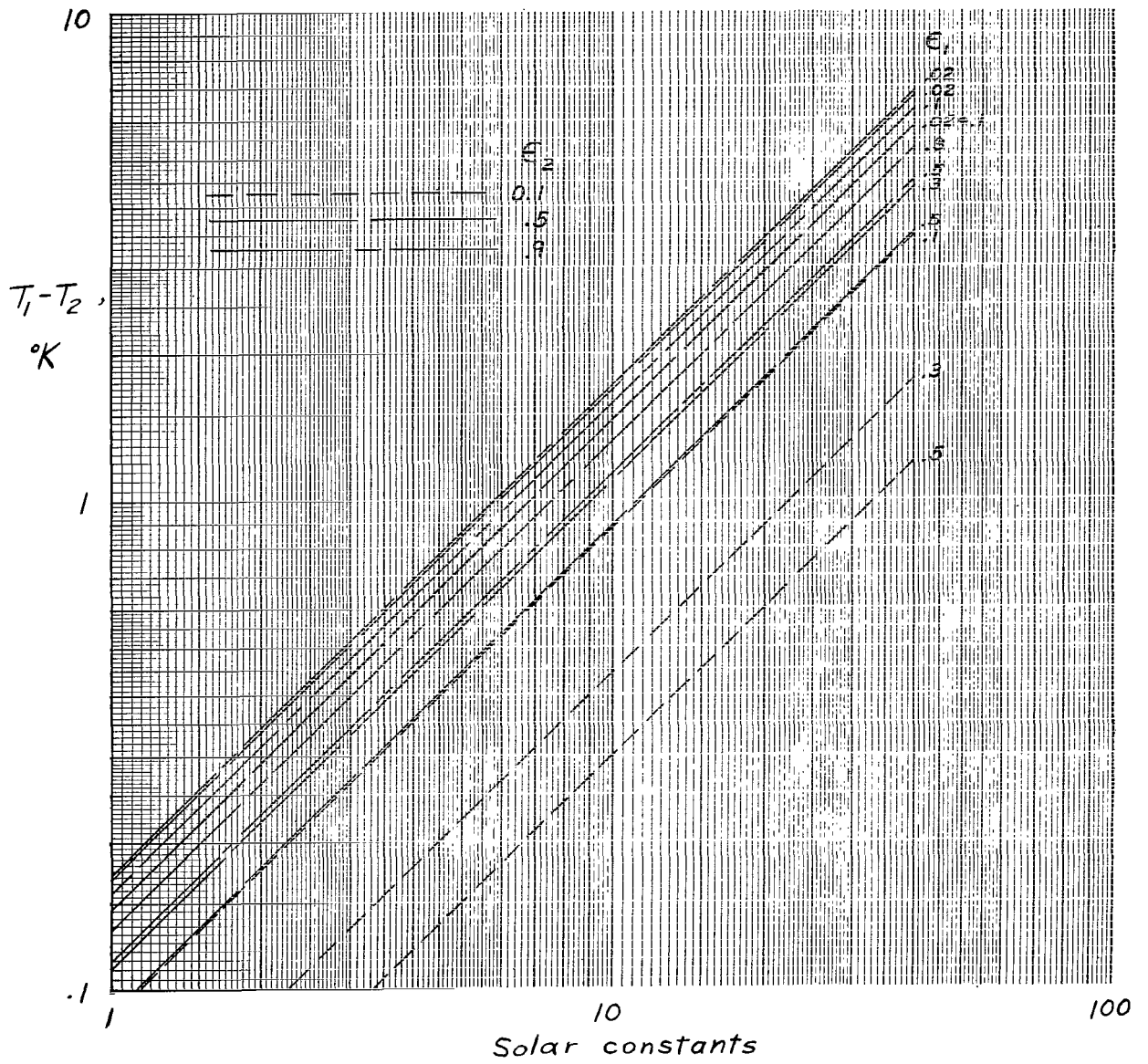


(a) $\frac{k}{t} = 10$.

Figure 17.- Temperature difference between front and rear surfaces of paraboloidal mirror for solar-probe case. $\alpha_1 = 0.125$; $\theta_R = 60^{\circ}$.

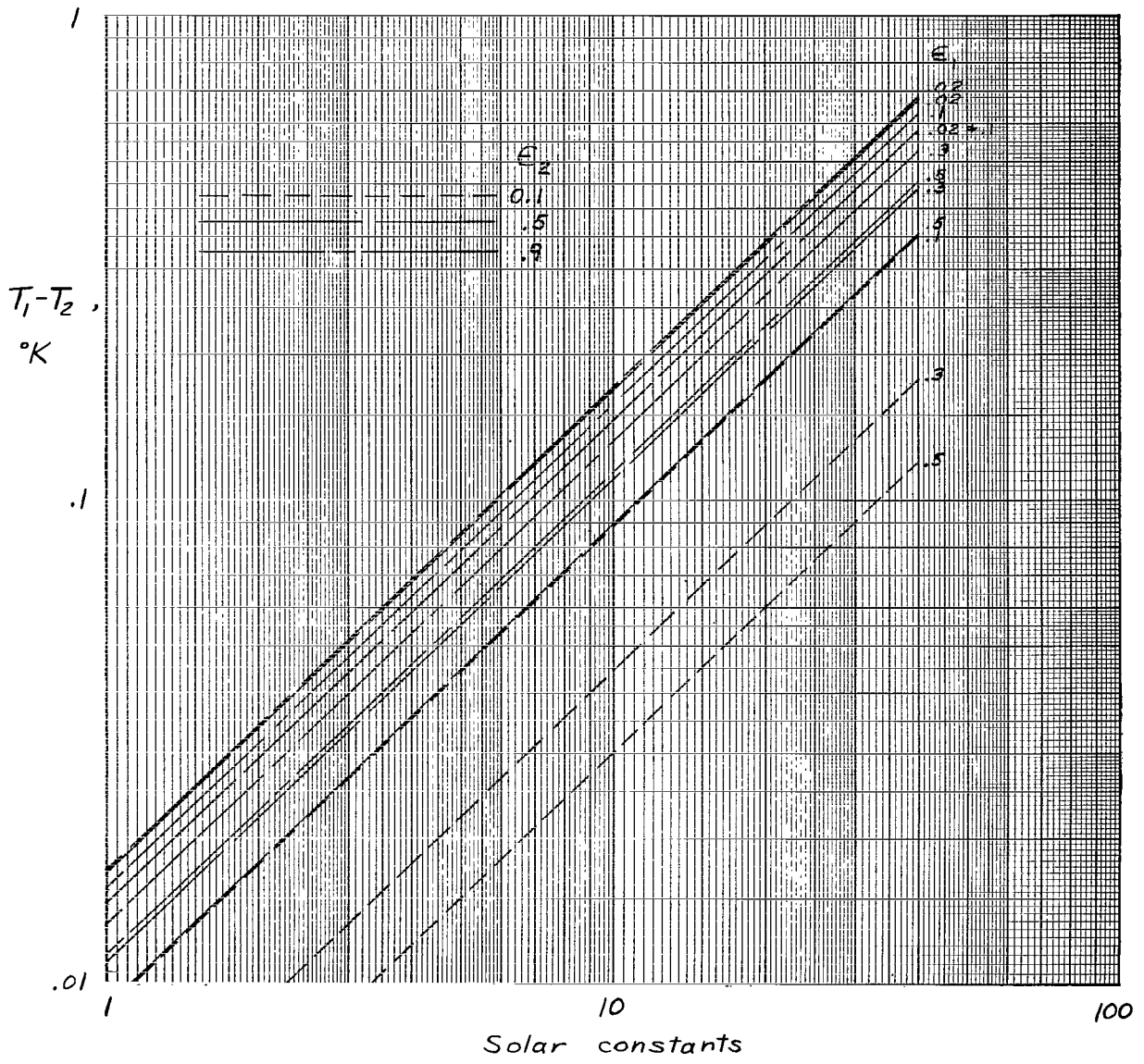


(b) $\frac{k}{t} = 100$.
 Figure 17.- Continued.



(c) $\frac{k}{t} = 1000$.

Figure 17.- Continued.



(d) $\frac{k}{t} = 10\ 000.$

Figure 17.- Concluded.

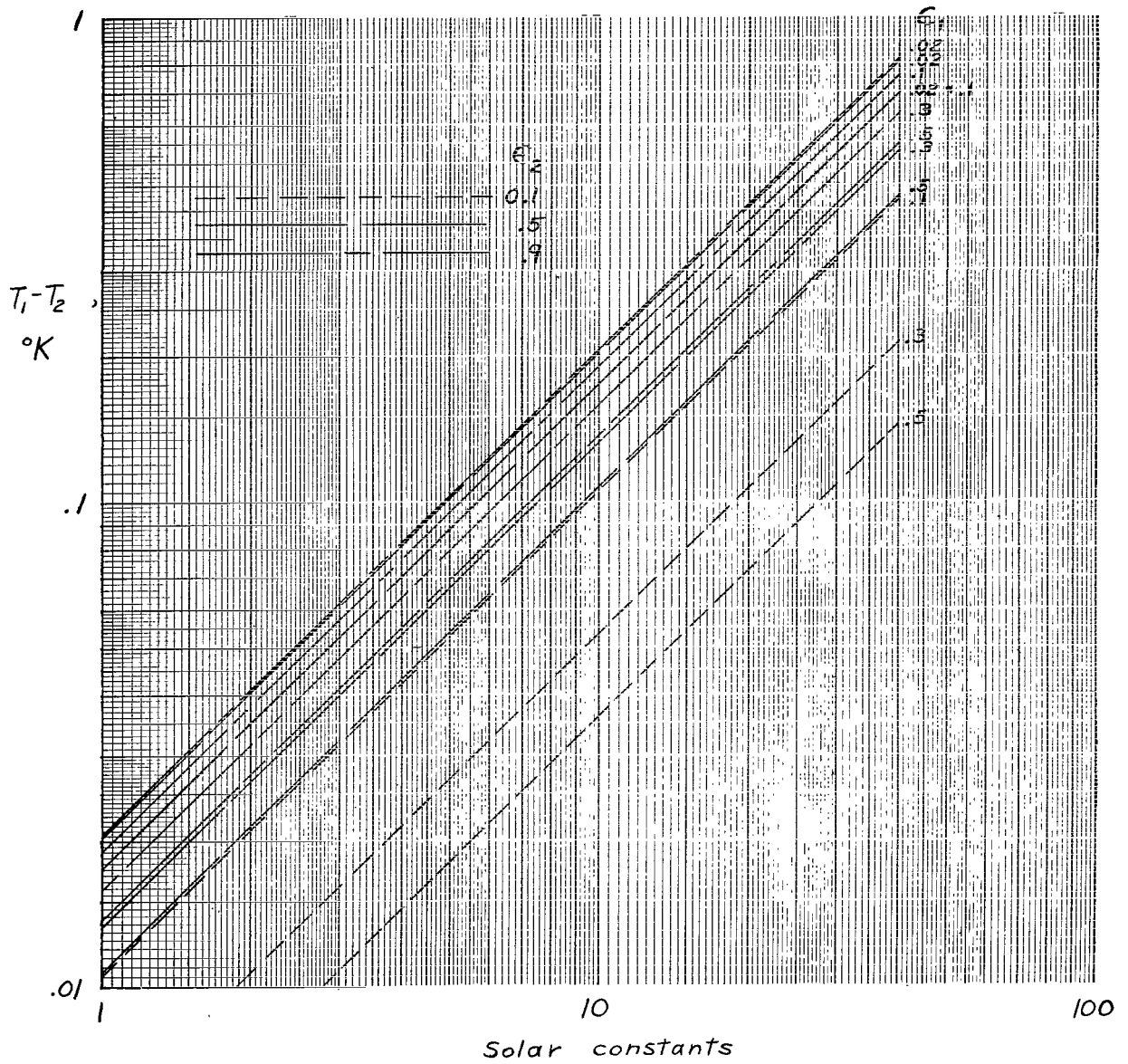


Figure 18.- Temperature difference between front and rear surfaces of paraboloidal mirror for solar-probe case. $\alpha_1 = 0.15$; $\frac{k}{t} = 10\ 000$; $\theta_R = 60^{\circ}$.

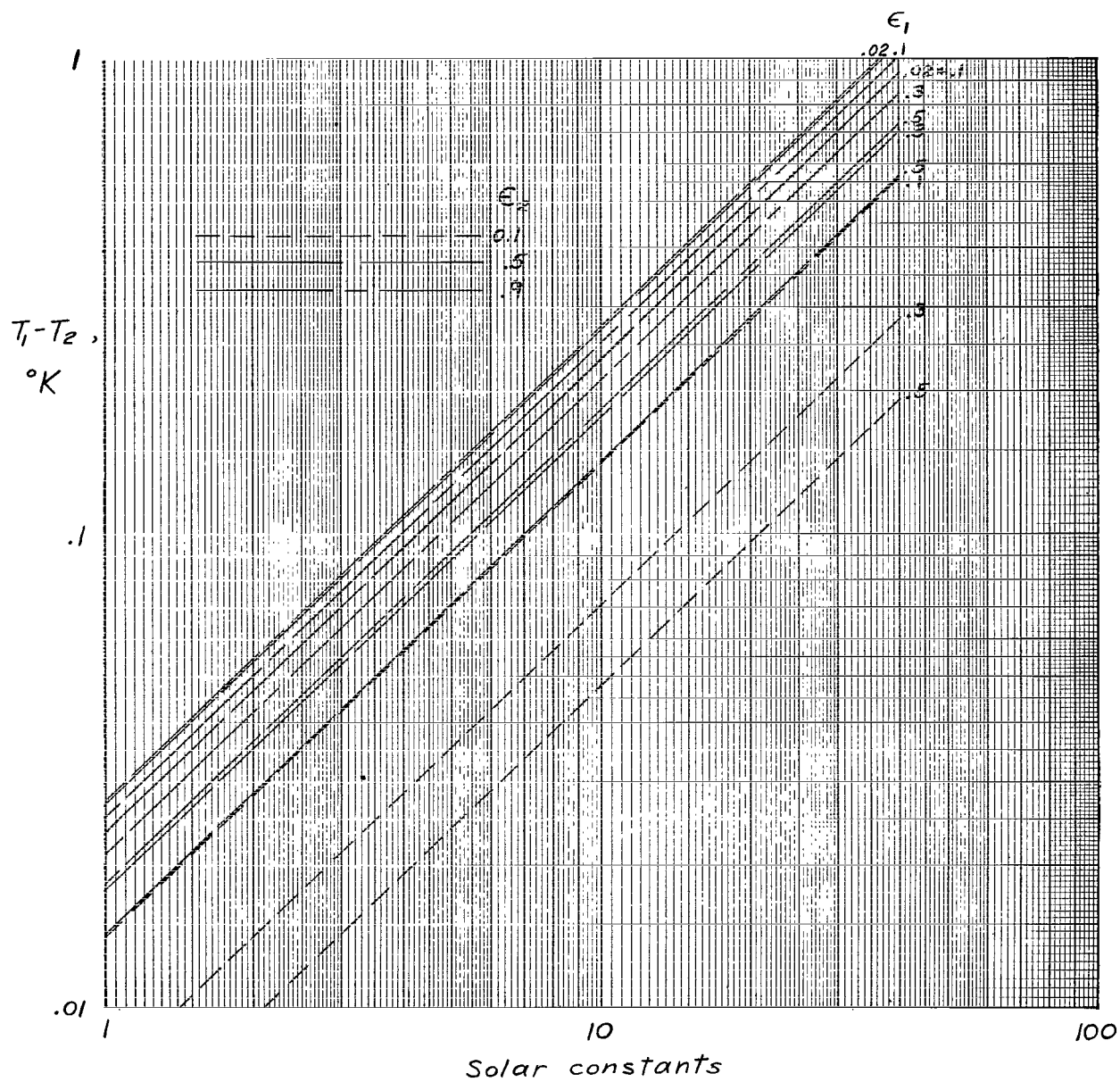


Figure 19.- Temperature difference between front and rear surfaces of paraboloidal mirror for solar-probe case. $\alpha_1 = 0.2$; $\frac{k}{r} = 10\ 000$; $\theta_R = 60^{\circ}$.

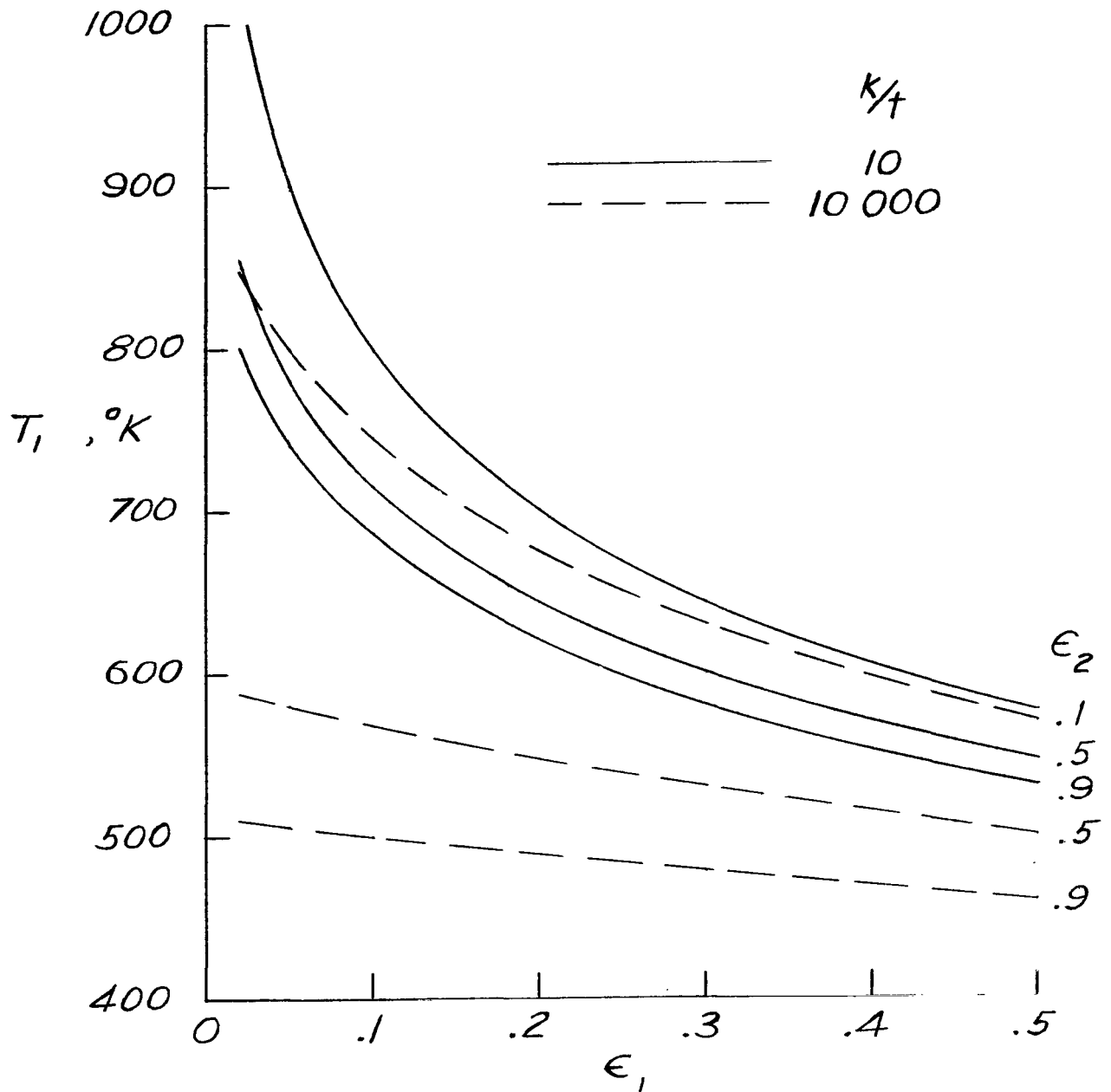


Figure 20.- Front-surface temperature of paraboloidal mirror at 20 solar constants. $\alpha_1 = 0.125$; $\theta_R = 60^\circ$.

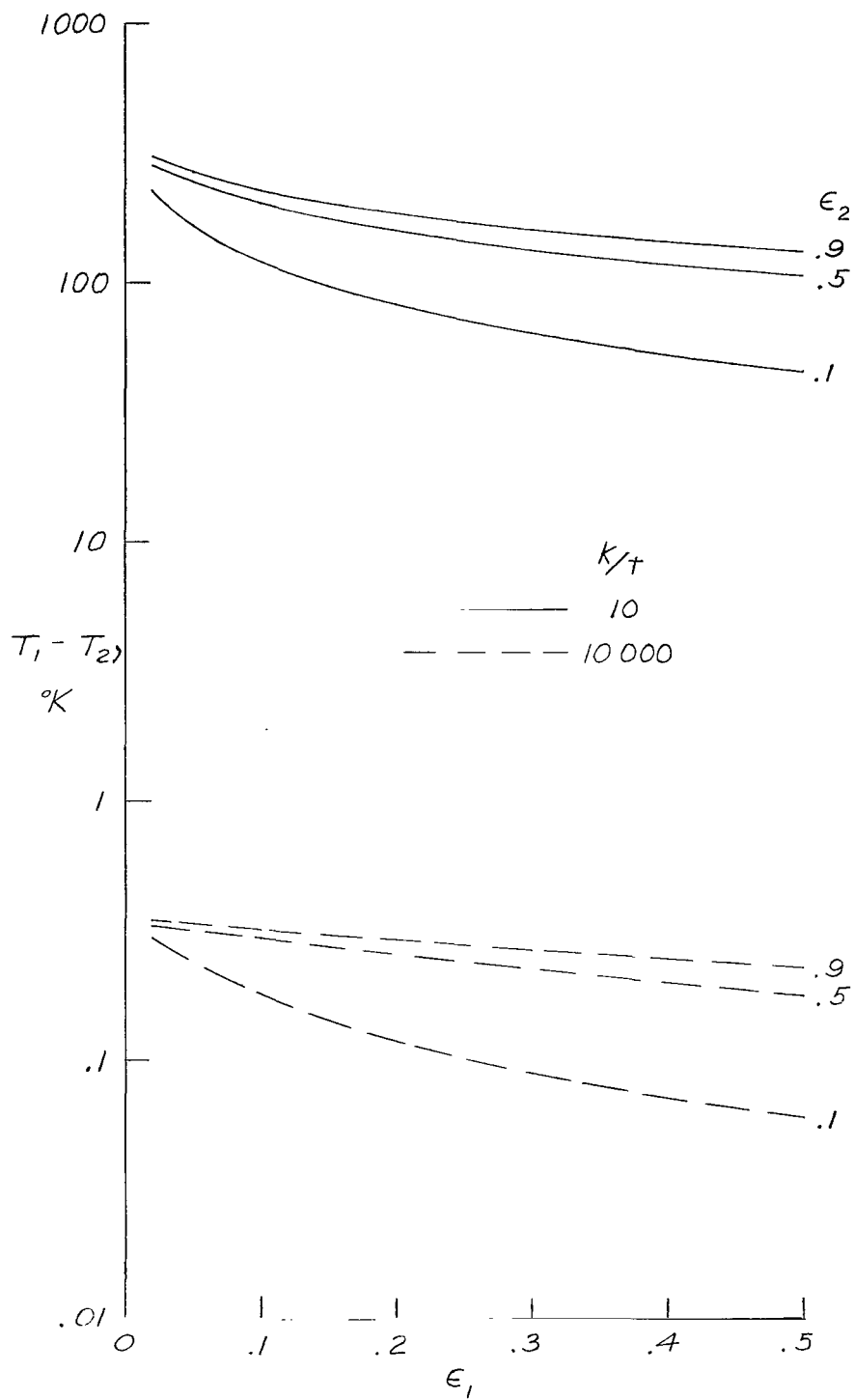


Figure 21.- Temperature difference between front and rear surfaces of paraboloidal mirror at 20 solar constants. $\alpha_1 = 0.125$; $\theta_R = 60^\circ$.

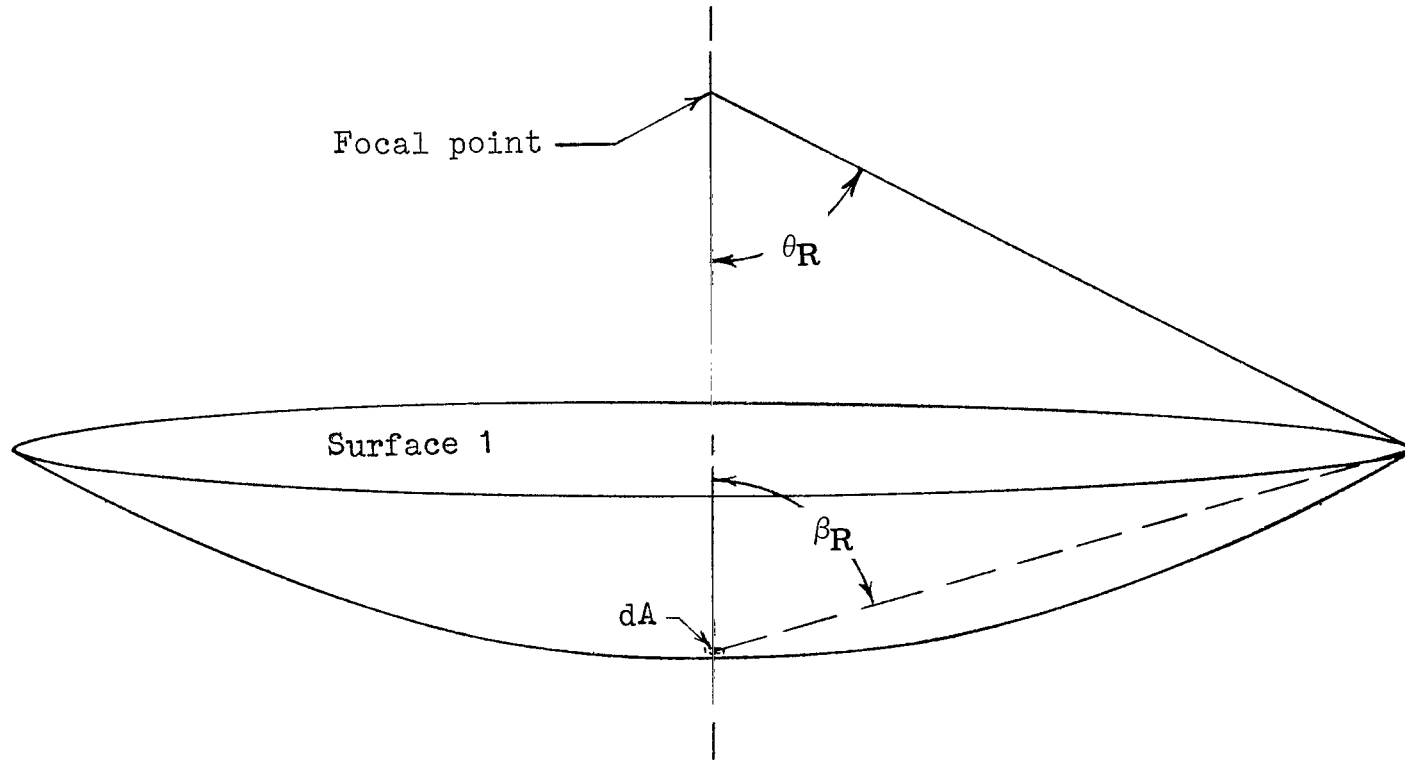


Figure 22.- Sketch of paraboloidal mirror for derivation of E_m .

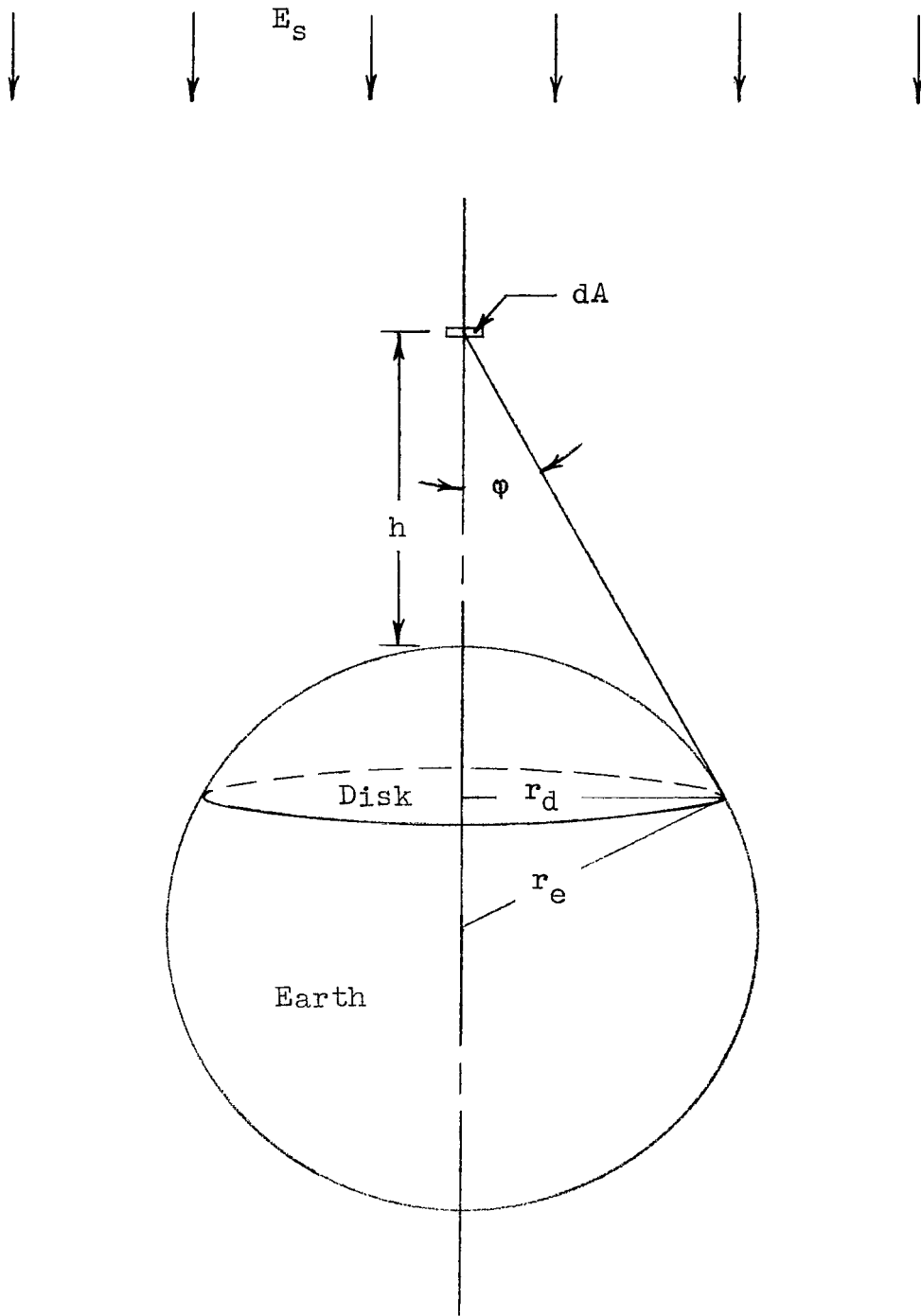


Figure 23.- Geometrical relation between mirror and earth.

FIRST CLASS MAIL

00100 00903
AFWL /
MEXICO 87117
CHIEF TECH. LIB

POSTMASTER: If Undeliverable (Section 158
Postal Manual) Do Not Return

"The aeronautical and space activities of the United States shall be conducted so as to contribute . . . to the expansion of human knowledge of phenomena in the atmosphere and space. The Administration shall provide for the widest practicable and appropriate dissemination of information concerning its activities and the results thereof."

— NATIONAL AERONAUTICS AND SPACE ACT OF 1958

NASA SCIENTIFIC AND TECHNICAL PUBLICATIONS

TECHNICAL REPORTS: Scientific and technical information considered important, complete, and a lasting contribution to existing knowledge.

TECHNICAL NOTES: Information less broad in scope but nevertheless of importance as a contribution to existing knowledge.

TECHNICAL MEMORANDUMS: Information receiving limited distribution because of preliminary data, security classification, or other reasons.

CONTRACTOR REPORTS: Scientific and technical information generated under a NASA contract or grant and considered an important contribution to existing knowledge.

TECHNICAL TRANSLATIONS: Information published in a foreign language considered to merit NASA distribution in English.

SPECIAL PUBLICATIONS: Information derived from or of value to NASA activities. Publications include conference proceedings, monographs, data compilations, handbooks, sourcebooks, and special bibliographies.

TECHNOLOGY UTILIZATION PUBLICATIONS: Information on technology used by NASA that may be of particular interest in commercial and other non-aerospace applications. Publications include Tech Briefs, Technology Utilization Reports and Notes, and Technology Surveys.

Details on the availability of these publications may be obtained from:

SCIENTIFIC AND TECHNICAL INFORMATION DIVISION
NATIONAL AERONAUTICS AND SPACE ADMINISTRATION
Washington, D.C. 20546